Theses and Dissertations | 1. Thesis and Dissertation Collection, all items

1983-06

Excitation frequency dependence of conductivity of electrolytic solutions.

Kolbeck, John Benedict

http://hdl.handle.net/10945/19801

NAVAL POSTGRADUATE SCHOOL
Monterey, California

THESIS

EXCITATION FREQUENCY DEPENDENCE OF
CONDUCTIVITY OF ELECTROLYTIC SOLUTIONS

by

John Benedict Kolbeck

June 1983

Thesis Advisor: J. Neighbours

Approved for public release; distribution unlimited

SECURITY CLASSIFICATION OF THIS PAGE (When Data Entered)

REPORT DOCUMENTATION PAGE		READ INSTRUCTIONS BEFORE COMPLETING FORM
1. REPORT NUMBER	2. GOVT ACCESSION NO.	3. RECIPIENT'S CATALOG NUMBER
4. TITLE (and Subtitle) Excitation Frequency Dependence of Conductivity of Electrolytic Solutions		5. TYPE OF REPORT & PERIOD COVERED Master's Thesis June 1983
		6. PERFORMING ORG. REPORT NUMBER
7. AUTHOR(s) John Benedict Kolbeck		8. CONTRACT OR GRANT NUMBER(s)
9. PERFORMING ORGANIZATION NAME AND ADDRESS Naval Postgraduate School Monterey, California 93940		10. PROGRAM ELEMENT, PROJECT, TASK AREA & WORK UNIT NUMBERS
11. CONTROLLING OFFICE NAME AND ADDRESS Naval Postgraduate School Monterey, California 93940		12. REPORT DATE June 1983
		13. NUMBER OF PAGES 88
14. MONITORING AGENCY NAME & ADDRESS(If different from Controlling Office)		15. SECURITY CLASS. (of this report) Unclassified
		15a. DECLASSIFICATION/DOWNGRADING SCHEDULE

16. DISTRIBUTION STATEMENT (of this Report)

Approved for public release; distribution unlimited

17. DISTRIBUTION STATEMENT (of the abstract entered in Block 20, if different from Report)

18. SUPPLEMENTARY NOTES

19. KEY WORDS (Continue on reverse side if necessary and identify by block number)

conductivity, frequency dependence
salt solutions - frequency dependence of conductivity

20. ABSTRACT (Continue on reverse side if necessary and identify by block number)

The frequency dependence of the electrolytic conductivity was studied for solutions of varying concentrations of NaCl, MgS04, KCl, and KBr. An experimental test fixture was designed and an equivalent electrical model of the test system developed. A theoretical model of the conductivity that accounts for charge carrier inertia is proposed. Measured

(continued)

DD FORM 1473 JAN 73   EDITION OF 1 NOV 65 IS OBSOLETE

S/N 0102- LF- 014- 6601

1

Item 20. (continued)

values of the impedance at various frequencies were used to
generate test system model parameters, and subsequently
identify sample response. Interpretation of the sample
response using the conductivity model allowed determination
of the conductivity, which is presented in the form of
the D.C. value or real part, Ko and the non-dielectric time
constant, Tc. The conductivity of the solutions decreased
with increasing frequency and the initial measurements of
Tc were of the order of nanoseconds. Variations in Ko with
salinity were in agreement with the empirical formula of
Walden.

Excitation Frequency Dependence of Conductivity
of Electrolytic Solutions

by

John Benedict Kolbeck
Lieutenant, United States Navy
B.S., United States Naval Academy, 1976

ABSTRACT

The frequency dependence of the electrolytic conductivity was studied for solutions of varying concentrations of NaCl, MgSO4, KCl, and KBr. An experimental test fixture was designed and an equivalent electrical model of the test system developed. A theoretical model of the conductivity that accounts for charge carrier inertia is proposed. Measured values of the impedance at various frequencies were used to generate test system model parameters, and subsequently identify sample response. Interpretation of the sample response using the conductivity model allowed determination of the conductivity, which is presented in the form of the D.C. value or real part, Ko and the non-dielectric time constant, Tc. The conductivity of the solutions decreased with increasing frequency and the initial measurements of Tc were of the order of nanoseconds. Variations in K with salinity were in agreement with the empirical formula of Walden.

TABLE OF CONTENTS

LIST OF TABLES

LIST OF FIGURES

ACKNOWLEDGEMENTS

I. INTRODUCTION

Extensive research has been directed at examining the
propagation of electromagnetic radiation in all environments.
Of fundamental concern to the Navy has been propagation
through its environment; the atmosphere, the air-ocean
interface and the ocean itself. Investigations concerning
ocean electromagnetics require an understanding of seawater
conductivity, or more fundamentally, electrolytic conductivity.
Historically, electrolytic conductivity research has been
divided into two areas; low frequency research using
frequencies below 10kHz, and high frequency experiments
utilizing frequencies above 10Mhz which probe the dielectric
nature of the solutions.

In this thesis, the frequency dependence of the electro-
lytic conductivity is observed between 10kHz and 10MHz by
measuring its impedance. The salt solutions examined are
the dominant contributors to seawater conductivity.
Sections II and III present current theory and model
development. Sections IV and V describe the experiment
and present an analysis of the results. Section VI
concludes with a summary and some possible areas for future
investigation.

II. BACKGROUND

An extensive literature search was carried out utilizing general chemistry reference material, textbooks, and computer methods. The Chemistry, Ocean Sciences, Geophysics and Electrical Engineering data banks of the DIALOG (Lockheed Data Base) computer information system contain information dating from approximately 1967. Systematic pursuit of the reference materials and their associated bibliographies/references consistently lead to the Debye-Falkenhagen model of conductivity proposed in 1928 [Ref. 1]. Harned and Owen [Ref. 2] (1963) along with Condon and Odishaw [Ref. 3] (1963) state Falkenhagen's theory and its historical verification. Smedley [Ref. 4] (1980) describes improvements to the Debye-Falkenhagen theory that occurred in the 1970's, but these newer theories apply to low concentration solutions in the low frequency regime (less than 10 kHz) only. Thus, the most recent model that describes the excitation frequency dependence of conductivity was published in 1928.

The model for Falkenhagen's conductivity theory is that of a hard sphere ion under the influence of an applied electric field drifting in a viscous and permeable medium [Ref. 5]. The reduction in mobility as concentration is increased is due to coulombic interactions between ions, the predominant effects being relaxation and electrophoresis.

An ion of charge Q is surrounded by ions whose net charge is -q. When an external electric field is applied, the central ion will be attracted to the electrode. Consequently, the previously spherically symmetric field around the central ion becomes asymmetric, for it cannot "relax" fast enough to follow the motion of the central ion toward the electrode. This creates a small force, the relaxation force, which inhibits the mobility of the central ion. When an ion moves in an electrolytic solution, it tends to drag the local solvent molecules with it. Since anions and cations move in opposite directions, each ion is effectively moving against a stream of solvent molecules. The subsequent reduction in ion mobility by this effect, the electrophoretic effect, can be attributed to an electrophoretic force.

Falkenhagen has included the force due to the applied field, the Stoke's law hydrodynamic force for a hard sphere in a viscous continuum, the electrophoretic force and the relaxation force in developing an equation of motion for the ion. He does not include any inertia term and stated "...it is permissible to neglect the forces due to dynamical reactions in comparison to the viscosity forces." [Ref. 6]. The forces due to dynamical reactions represent the inertia of the ion in the solution, i.e. its inherent resistance to a change in velocity. Falkenhagen qualified his statement by comparing the two forces and showing that the viscosity force was larger than the inertial force. Two assumptions

critical to his argument concern the charge carriers, specifically the size (radius) and mass. In view of present uncertainty as to the methods and mechanisms of charge transport, the validity of Falkenhagen's assumptions are suspect. The absence of this inertia term lead to a real expression for the conductivity. Falkenhagen's relaxation force is inversely proportional to the frequency of the applied electric field, and decreased with increased frequency. Consequently, he stated that conductivity will increase with increasing frequency for the ion is more mobile. Experimental data supporting this theory was collected by Sack [Ref. 7] and other investigators and summarized by Geest [Ref. 8]. Careful examination of these experiments, all performed in the late 1920's, revealed that they were relative measurements obtained by recording the difference in response of both the test cell and solution at various frequencies using a bridge network. Additionally, the measurements were subject to sizeable experimental uncertainties (of the same magnitude as the measured parameter) due to the sensitive nature of the measurement and the available technology. Thus, the results from these experiments required careful interpretation and were based heavily on existing theory.

Retaining the inertia term in the equation of motion results in a complex form for the conductivity, and is developed in section III. As the frequency is increased,

the imaginary part of the conductivity becomes smaller. The
net effect is a decrease in conductivity with frequency.

III. <u>THEORY</u>

This section presents the theoretical foundation upon which the experiment was conducted. Part A presents the fundamental development starting from Maxwell's equations. Part B develops the expression for the conductivity and Part C describes the specific application to this experiment.

A. FUNDAMENTAL BACKGROUND

Maxwell's equations for time harmonic fields can be expressed as:

$$\nabla \times \overline{B} = \mu \overline{J} + \mu j \omega \overline{D} \quad ; \quad \nabla \times \overline{E} = -j \omega \overline{B}$$

$$\nabla \times \overline{D} = \rho \quad ; \quad \nabla \cdot \overline{B} = 0$$

the constituative relationships are:

$$\overline{J} = K\overline{E} \quad ; \quad \overline{B} = \mu \overline{H}$$

$$\overline{D} = \varepsilon \overline{E} = \varepsilon_0 \overline{E} + \overline{P} = \varepsilon_0 \overline{E} + \varepsilon_0 x \overline{E} = \varepsilon_0 (1 + \chi) \overline{E} \quad \text{where,}$$

K is the electrical conductivity, $\chi = x' - jx''$ is the complex susceptibility and $\varepsilon = \varepsilon_0 (1 + \chi)$ is the complex permativity. After substitution, Maxwell's equations reduce to:

$$\nabla \quad \overline{B} = \mu o (K + j\omega \varepsilon) \overline{E} = \mu o \; j \; \hat{\varepsilon} \; \overline{E}$$

$$\nabla \quad \overline{E} = -j \varepsilon \overline{B} \quad ; \nabla \cdot \overline{B} = 0$$

$$\nabla \cdot \hat{D} = \hat{\rho} \quad ; \quad \hat{\varepsilon} = \varepsilon \left(1 + \frac{K}{j\omega\varepsilon}\right)$$

$$\hat{D} = \hat{\varepsilon} \; \overline{E} \quad ; \quad \hat{\rho} = \hat{\varepsilon} \nabla \cdot \overline{E} = \varepsilon \nabla \cdot \overline{E} + \frac{K}{j\omega} \nabla \cdot \overline{E}$$

14

where the effective quantities (denoted by ^) have been
introduced for computational ease. This formulation is
typically used in problems involving conducting dielectrics.
To more clearly distinguish between dielectric and conductor
properties, several specific cases are examined.

    1. <u>Case 1</u>

      Consider a conducting, lossy dielectric medium
between two parallel plates. Using the effective notation,
the impedance of this device is:

$$z \;=\; \frac{1}{j\omega \hat{c}} \quad \text{where}$$

$$\hat{c} \;=\; \frac{\int \hat{\varepsilon}\overline{E}\cdot d\overline{s}}{-\int \overline{E}\cdot d\ell} \;=\; \hat{\varepsilon}\,\frac{A}{\ell} \qquad \begin{array}{l} A = \text{plate surface area} \\ \ell = \text{plate separation} \end{array}$$

and $\qquad \hat{\varepsilon} \;=\; \varepsilon\left(1 + \dfrac{K}{j\omega\varepsilon}\right)$

Therefore the impedance (in conventional notation) is:

$$z \;=\; \frac{1}{j\omega\hat{\varepsilon}\frac{A}{\ell}} \;=\; \frac{1}{j\omega\,\frac{A}{\ell}\left(\varepsilon - \frac{jK}{\omega}\right)}$$

This result could be generated by a more conventional approach.
The medium can be characterized by a capacitor in parallel
with a resistor. The impedance is:

$$z \;=\; \frac{1}{j\,\omega c + G} \qquad \text{where} \quad c \;=\; \frac{\varepsilon A}{\ell} \quad \text{and}$$

$$G \;=\; \frac{KA}{\ell}$$

so that:

$$z \;=\; \frac{1}{j\omega\varepsilon\,\frac{A}{\ell} + \frac{KA}{\ell}} \;=\; \frac{1}{j\omega\frac{A}{\ell}\left(\varepsilon + \frac{K}{j\omega}\right)}$$

$$= \frac{1}{j\omega\frac{A}{\ell}(\varepsilon - j\frac{K}{\omega})}$$

which is identical to the earlier result. Incorporating the constituative equations, which are:

$$\varepsilon = \varepsilon_0 (1 + X) = \varepsilon' - j\varepsilon'' \quad \text{and}$$

$$X = x \quad - jx'$$

the impedance of the device can be expressed as:

$$z = \frac{1}{j\omega\frac{A}{\ell} \varepsilon' + \frac{A}{\ell}(\omega\varepsilon_0 x'' + K)} \tag{1}$$

2. <u>Case II</u>

Consider a finite conductor between two parallel plates. The impedance is purely resistive and of the form:

$$z = R = \frac{\ell}{AK} \tag{2}$$

ℓ = length of conductor

A = conductor cross-sectional area

K = electrical conductivity

3. <u>Case III</u>

Consider a non-conducting lossy dielective between two parallel plates. The impedance is:

$$z = \frac{1}{j\omega c} = \frac{1}{j\omega \frac{A}{\ell}(\varepsilon' - j\varepsilon'')} \tag{3}$$

where

$$c = \frac{\int \varepsilon\overline{E}\cdot d\overline{s}}{\int \overline{E}\cdot d\ell} = \varepsilon\frac{A}{\ell} = (\varepsilon' - j\varepsilon')\frac{A}{\ell}$$

16

B. CONDUCTIVITY MODEL

A standard definition for conductivity is:

$$K = p+ \; u+ \; + \; p- \; u- \tag{4}$$

where $p+,-$ is the charge density of the $+,-$ ion and $u+,-$ is the charge mobility of the $+,-$ ion. The mobility of the ion can be obtained following Jackson [Ref. 10]:

$$u = \frac{<v>}{E} \tag{5}$$

$$m \frac{d<v>}{dt} + mb<v> = qE \tag{6}$$

where $<v>$ is the mean velocity of the ion, m is the mass, b is a damping constant that reflects the change in ion velocity due to collisions, q is the charge of the ion, and E is the applied electric field. Only one dimensional motion will be considered. Let $<v>$ and E have the time harmonic form $\exp(j\omega t)$. Then, solving equations (5) and (6) we obtain

$$u = \frac{Uo}{1+j(\omega/b)} \qquad \text{where} \quad Uo = \frac{q}{mo} \tag{7}$$

Substituting equation (7) into equation (4), the expression for conductivity becomes:

$$\tag{8}$$

$$K = \frac{p+Uo+}{1 + j\frac{\omega}{b+}} \quad + \quad \frac{p-Uo-}{1 + j\frac{\omega}{b-}}$$

Considering the simple salts of interest, such as NaCl, we can assume p+ = p- = p. Additionally, given equal anion-cation charge magnitudes, the damping forces are assumed to be similar. Therefore, b+ = b- = b. Applying these two simplifications, the expression for the conductivity, from Becker [Ref. 11], becomes:

$$K = \frac{[p(Uo+ + Uo-)]}{1 + j\frac{\omega}{b}} = \frac{Ko}{1 + j\frac{\omega}{b}}$$

where   Ko = p(Uo + Uo-)

C.   APPLICATION

The experiment dealt with simple salt solutions which could be considered as conducting, lossy, dielectric media. The test fixture, described in Section III, can be modeled as two parallel plates. Therefore, the impedance of the test circuit can be interpreted as that derived in case I using equations (2) and (3). Incorporating the expression for the complex conductivity, the impedance of a conducting, lossy, dielectric medium between paralle plates becomes:

$$Z = (j\frac{\omega A \varepsilon'}{\ell} + \frac{A}{\ell}\omega\varepsilon'' + \frac{AK}{\ell})^{-1}$$

$$= (j\frac{\omega A \varepsilon}{\ell}' + \frac{A}{\ell}\omega\varepsilon'' + \frac{A}{\ell}\frac{Ko}{(1 + j\omega/b)})^{-1}$$

$$= (j\omega\varepsilon'' + j\omega\varepsilon' + \frac{1}{\frac{\ell}{AKo} + j\omega\frac{\ell}{AKob}})^{-1}$$

$$= (j\omega\varepsilon'' + j\omega C + \frac{1}{R + j\omega L})^{-1}$$

where
$$R = \frac{\ell}{AKo} \quad \text{and} \quad L = \frac{R}{b}$$

Since this research considered only aqueous solutions, and utilized frequencies below 10 MHz, several simplifications can be made. From Kittle [Ref. 12], the dielectric constant of water at room temperature is given by:

$$\varepsilon' = 1 + \frac{4\pi aN}{1 + (\omega t)^2} \cong 80$$

where a is the static orientational polarizability, t the dielectric relaxation time $\cong 10^{-11}$, and N the number of spherically shaped molecules. For $\omega \cong 10^8$, we have $(\omega t) \cong 10^{-3}$ so that:

$$\varepsilon' = 1 + \frac{4\pi aN}{1 + (10^{-3})^2} \cong 1 + 4\pi aN \cong 80$$

and is independent of frequency. Thus, $4\pi aN \cong 79$. Also from Kittel [Ref. 13], the complex dielectric constant is:

$$\varepsilon = \varepsilon' - j\varepsilon'' = 1 + \frac{4\pi aN}{1 + (\omega t)^2} - j\frac{4\pi aN t}{1 + (\omega t)^2}$$

If we compare the real and imaginary parts:

$$\frac{\varepsilon''}{\varepsilon'} = \frac{4\pi aN(\omega t)}{1 + (\omega t)^2 + 4\pi aN} \cong \frac{79(\omega t)}{1 + (\omega t)^2 + 79}$$

19

$$= \frac{79 \ (\omega t)}{80 + (\omega t)^2}$$

Now, for $\omega \leq 10^8$, and $t = 10^{-11}$ s; the ratio becomes:

$$\frac{\varepsilon''}{\varepsilon'} = \frac{79(10^{-11})}{80 + 10^{-22} \omega^2} \cong \frac{79(10^{-3})}{80 + (10^{-6})}$$

$$\cong 10^{-3}$$

As decreases, ε'' gets smaller much faster than ε', and the difference between them grows. Therefore, we can neglect the ε'' term in the impedance equation.

The impedance becomes:

$$Z = (j\omega c + \frac{1}{R + j\omega L})^{-1}$$

This form of the impedance corresponds to the circuit model shown in Figure 1. The capacitor C reflects the effects of the solution in the conductivity cell. The resistor R and inductor L reflect the effect of the specific salt chosen as solute. The experiment consisted of measuring the value of C using distilled water and measuring the total impedance of the cell filled with sample. From this data, the values of R and L were calculated, and subsequently the value for b (b = R/L).

It is important to note that the ε'' term which was neglected in the impedance equation would correspond to a resistive effect in light of the proposed circuit model. It affects the real part, not the imaginary part of the

20

Figure 1. Electrical Equivalent Circuit
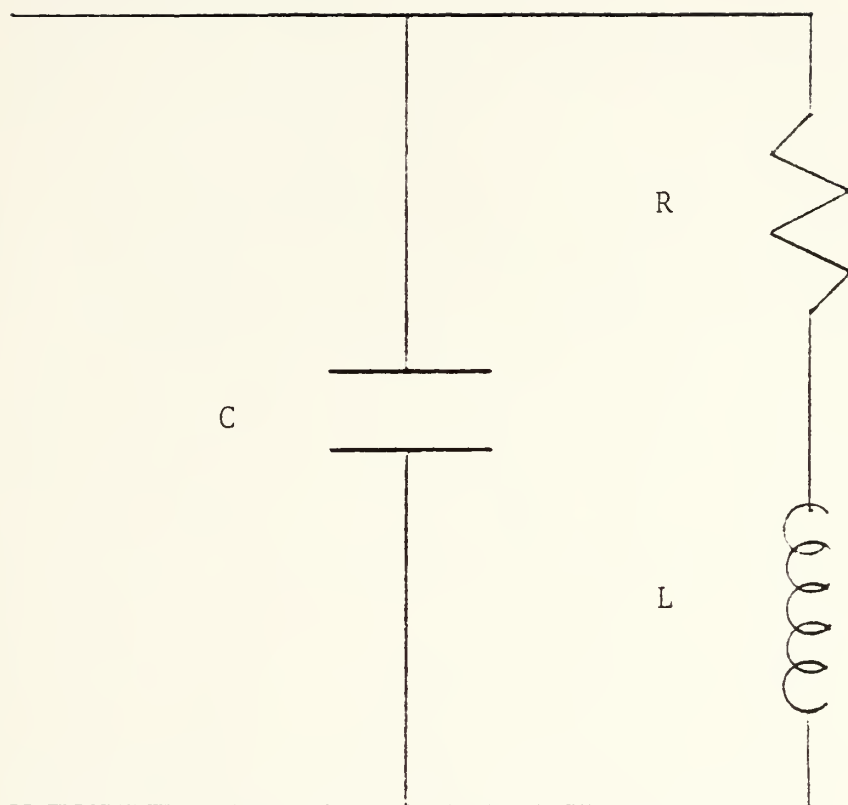
Figure 1. Electrical Equivalent Circuit

impedance. Thus, the sign of the phase angle (negative implying capacitive behavior; positive implying inductive behavior) would be determined by the other circuit elements.

IV.   EXPERIMENT

A.   APPARATUS

1.   Measurement System

Impedance measurements were made with the Hewlett-Packard (HP) Multi-Frequency LCR Meter (type 4275A, HP No. 2045J0]046) on loan from the Applied Physics Laboratory, The Johns Hopkins University. This instrument was calibrated by Hewlett-Packard 18 November 1982 using calibration standards traceable to the National Bureau of Standards to the extent allowed by the Bureaus' calibration facilities [Ref. 14]. Control of the LCR meter was through a Hewlett-Packard 85 Personal Computer (HP No. 2139A4139A) via the Hewlett-Packard Interface Bus.

The LCR meter is a microprocessor based impedance measuring instrument, [Ref. 15], which measures the vector impedance (or admittance) of the unknown sample to be tested. Ten test frequencies were available from the LCR meter: 10kHz, 20kHz, 40kHz, 100kHz, 200kHz, 400kHz, 1MHz, 2MHz, 4MHz, and 10MHz.

Connection of an unknown sample was as shown in Figure 2. A four terminal (HPOT, HCUR, LPOT, and LCUR on Figure 2) network was used to connect the LCR meter to the device under test (DUT). This terminal architecture limited the effects of mutual inductance, interference of

23
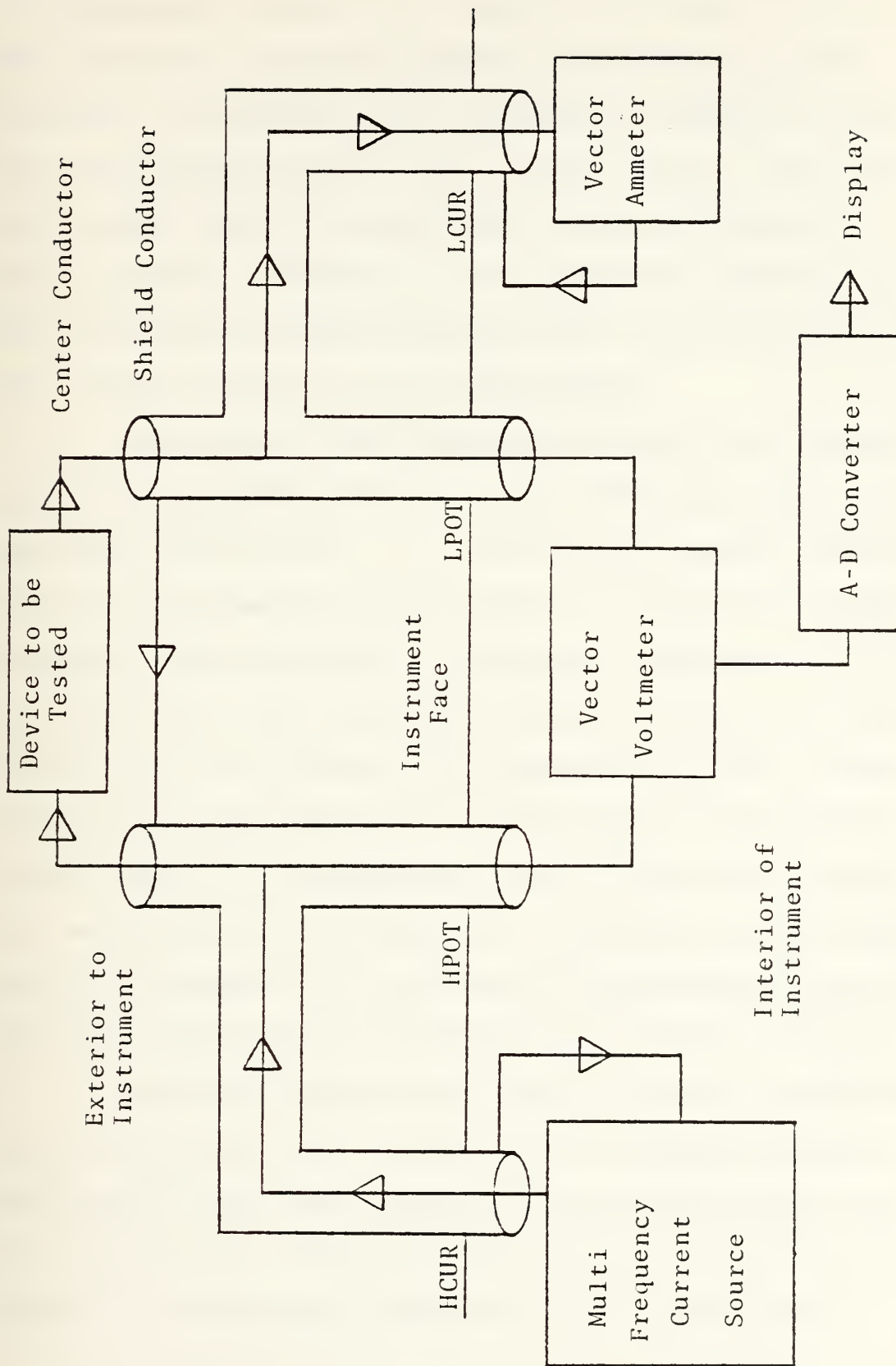
Figure 2. Measurement System Signal Flow

24

the measurement signals, and unwanted residual factors in the connections which are normally encountered in high frequency measurements. The measurement current utilized the outer shield conductor for a return path. Since the same current flowed through inner and outer conductors, but in opposite directions, no net inductive magnetic field was formed which ensured minimal error contribution by the test leads or fixture to the measurement.

Dependence of the measurement on the test fixture was also minimized by the use of the LCR meter zero offset adjustment (ZOA) [Ref. 15]. The inductive and/or capacative nature of the complete test fixture was measured at each frequency. This was done in two steps, first by measuring the capacitance and conductance of the fixture in an open circuit state (e.g. empty, dry conductivity cell). Then the impedance and resistance of the fixture in the short circuit state (e.g. conductivity cell filled with mercury) were measured at each frequency. The meter retained these values and automatically performed optimum compensation on subsequent measurements to remove test fixture response.

The HP-85 computer was used to control the LCR meter via the interface bus. Several BASIC language programs were written that fully controlled the measurements taken on a given sample. This procedure ensured that the LCR meter setup (i.e. measurement parameter, test signal level,

frequency, etc.) was identical for each test data cycle. It also enabled a large number of measurements of a given parameter to be accomplished in a short amount of time.

2. Test Cells

Two test cells were used in this experiment. Cell #1 was a conventional conductivity cell as sketched in Figure 3.a. The borosicilate glass cell body held approximately 30ml and had 2 electrodes coated with platinum black. The electrode leads penetrated the cell wall through lime glass supports and a brass capped connection point. The cell constant is defined as the ratio of the separation distance to the surface area of the electrodes. The cell #1 cell constant of 1.19 1/cm was determined using the procedures of Reference 16. A solution consisting of .7466g KCl in 1KG of solution (KCl plus H20) was the standard. The resistance was measured using a LKB-PRODUKTER conductivity bridge (type LKB 3216B) calibrated 18 March 1983.

Test cell #2 is depicted in Figure 3.b. The cell was made of 5/16 inch ID thickwall TYGON tubing and two nylon "tee" connectors which provided fill and drain ports. The electrodes were made of 5/16 inch OD solid carbon rods machined such that the electrode face was flat and perpendicular to the axis of the rod. The electrodes were connected to the instrument test leads by means of machined brass clamps as shown in Figure 4. The cell constant of 27.38 1/cm for cell #2 was determined by comparison to
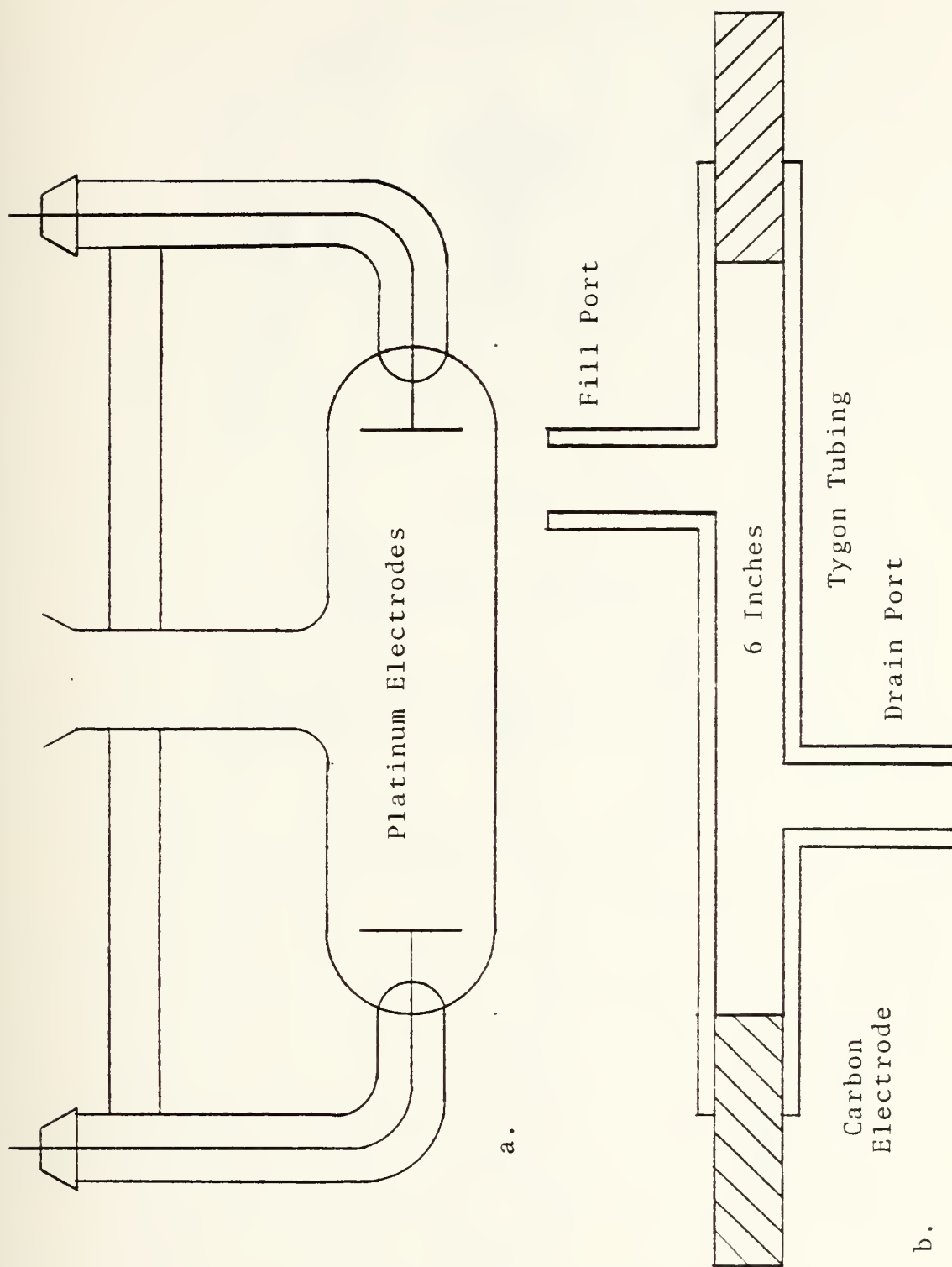
Figure 3. Experimental Conductivity Test Cells
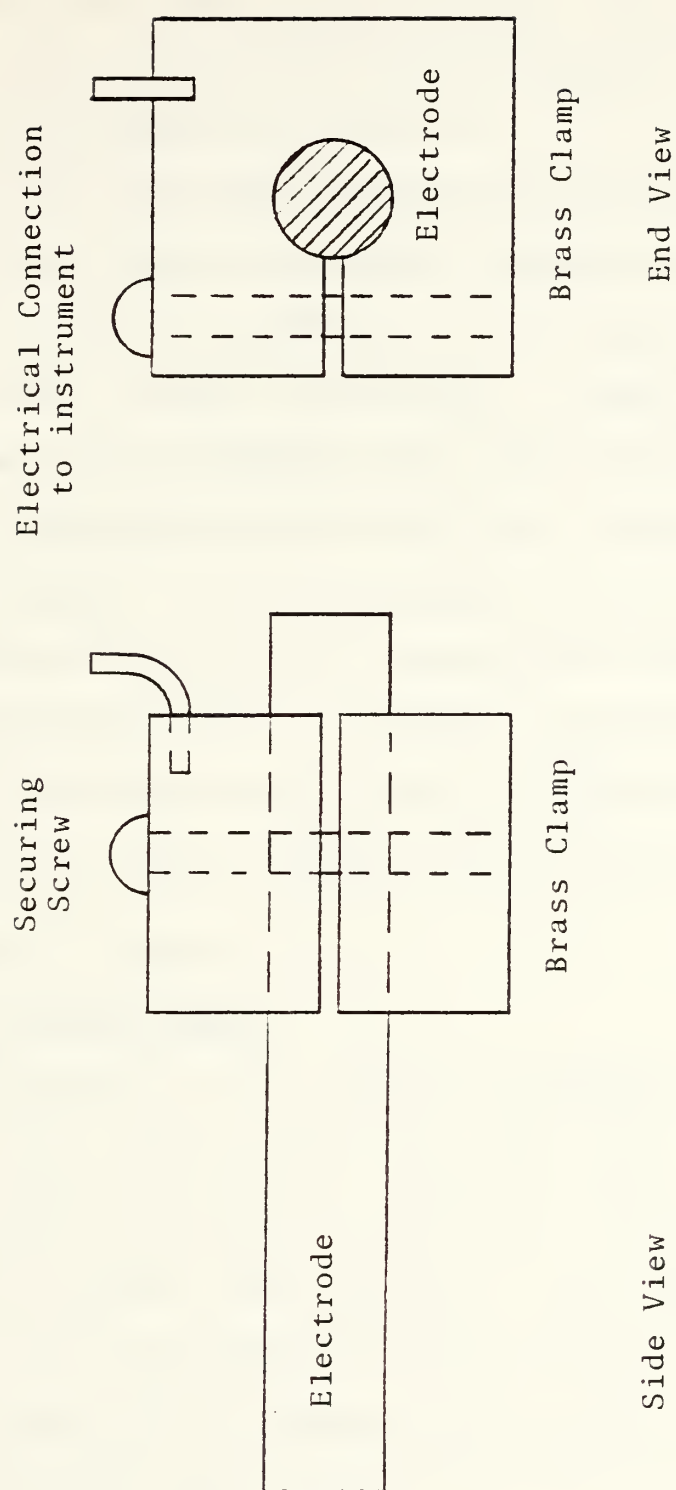
Figure 4.   Electrode Connection Clamp

cell cell #1; the value of conductivity for a specific
solution must be the same for both cells. This method was
used because cell #2, by virtue of its design, cannot be
thermostated as accurately as cell #1.

Each cell was supported and partially enclosed in
styrofoam. This support arrangement ensured no additional
electrical or magnetic pertubation of the measurement
and minimized any thermal fluctuations. Temperature measure-
ments were made with a WEKSLER (type 1509) immersion thermo-
meter. The experiment was performed in a relatively static
thermal environment. Early measurements of a variety of
solutions showed no appreciable temperature variation
during a measurement cycle. A constant temperature bath
was not utilized because of the static thermal environment
and the inductive effects observed due to bath operation/design.

B. EXPERIMENTAL APPROACH

1. Experimental Model

Determination of the solution parameters of interest
required that any effects due to the cell (test fixture)
be understood and eliminated if possible. To this end
the problem was divided into two parts: the physical test
fixture, and the equivalent electrical circuit simulating
the test solution and its interaction with the test fixture.

a. Physical Test Fixture

The test fixture consisted of the conductivity
cell and the leads connecting it to the measuring instrument.

29

Since the conductivity cell consisted of two flat electrode plates with a dielectric between them (primarily water) it was capacitive by nature. The test leads were approximately 6 inches each of RG-58C/U coaxial cable, and had a small resistance and inductance associated with them. Additionally there were several coaxial connector joints and solder joints, each with some residual effect. These accumulated effects were quite complex, but were essentially negated using the zero offset adjustment (ZOA) feature of the LCR meter. The ZOA was performed sequentially in two steps. The test fixture was assembled with the conductivity cell dry for the open circuit portion. Initiated by the "open" button, the meter automatically measured the capacitance and conductance at each test frequency. The cell was carefully filled with mercury and the short circuit portion of the ZOA initiated using the "short" button. The instrument automatically measured the inductance and resistance at each test frequency. The values were retained by the LCR meter and subsequent measurements were compensated to remove test fixture response. To identify and verify the remaining background of the test fixture, the inductance, resistance and vector impedance of the mercury were measured and recorded (see Appendix A).

Unfortunately, cell #1 did not have a drain port. It had to be physically disconnected to be drained and rinsed for each new test sample. This reconnection

altered the test fixture slightly, and could have introduced errors not accounted for in the initial ZOA. To identify these errors, the inductance, resistance, and vector impedance of mercury was measured after a reconnection and compared to readings after ZOA. As shown in Appendix A, post reconnection values were slightly greater than post ZOA values and were subsequently used to determine measurement accuracy. The open circuit portion of the ZOA was performed prior to each measurement run to partially compensate for the reconnection change.

b. Test Solution Equivalent Circuit

The equivalent electrical circuit of the test solution shown in Figure 5 was derived using the following considerations. The capacitor C reflected the general character of the conductivity cell; a parallel plate capacitor with a dielectric material between the plates. The dielectric material was the test solution, which was pre-dominantly water even at the higher concentrations. From Hasted [Ref. 17], the dielectric constant does depend on salinity, but this is a small effect and was subsequently ignored. Therefore, the value of C was determined reasonably accurately from the measured response of pure water as test solution.

The rest of the circuit in parallel with C represented the response of the solute and its interaction with the electrodes. The electrodes were interface surfaces
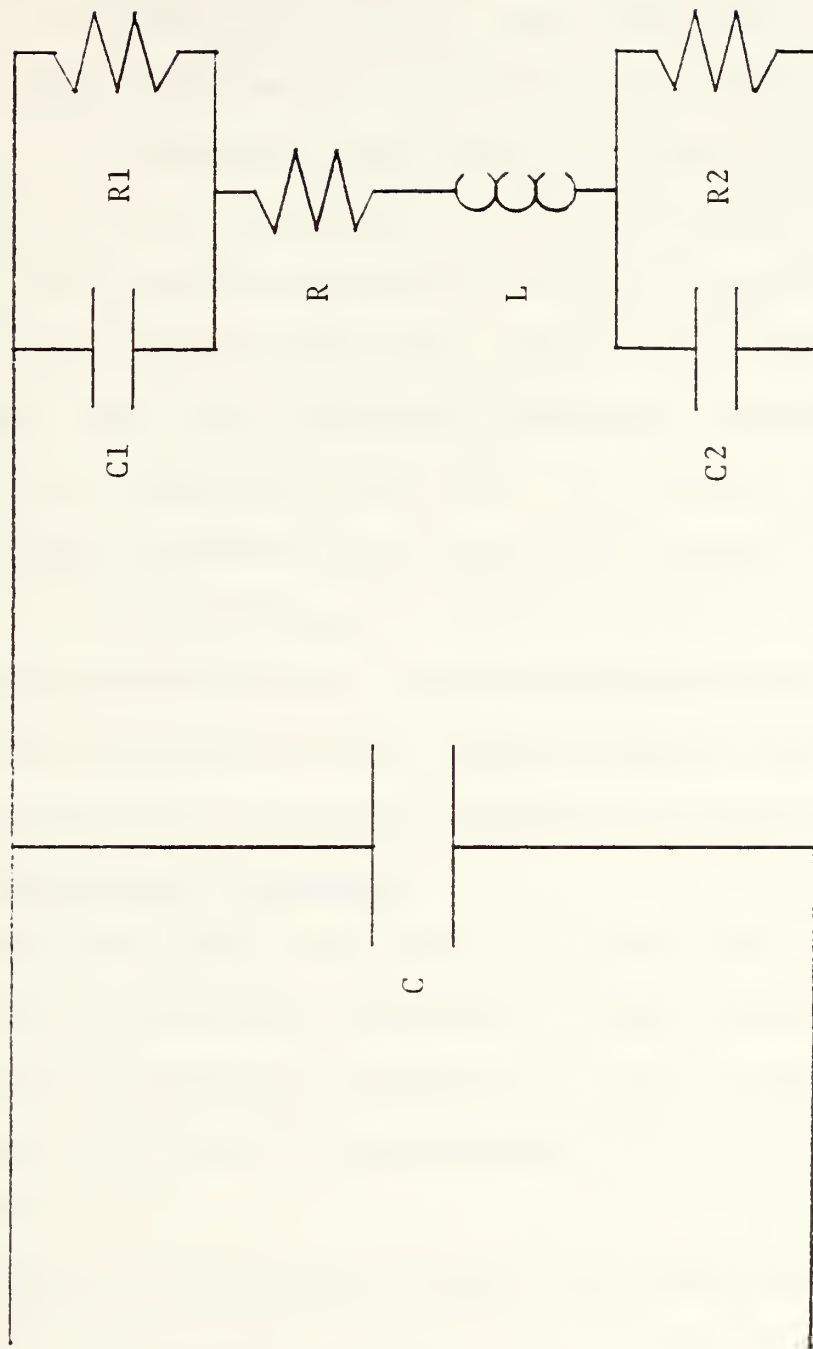
Figure 5. Equivalent Electrical Circuit

32

for the transition between electronic conduction and ionic conduction, and on a microscopic scale extremely complex. However, on a macroscopic scale, this transition effect was more simply modeled as a capacitor in parallel with a resistor. The capacitor reflected the dielectric layer which plated on the electordes, while the parallel leakage resistor reflected the imperfections in the layers and subsequent non-ideal capacitance. Since there were two electrodes, each with a different ion layer structure, each electrode was considered separately. $C1$, $R1$, $C2$, and $R2$ were the model parameters that described the two electrodes.

The remaining two elements, R and L, represented the response of the solute. As described earlier, R and L formed the expression for the complex conductivity, and were the parameters of primary interest in this research.

2. Measurement Procedure

The pure water and stock solutions were allowed several days to thermally stabilize in the laboratory. The LCR meter was energized 4-6 hours prior to any data runs. Just prior to a series of measurements, the ZOA was performed as follows:

1. Conductivity cell was drained and connected to the meter.

2. Open circuit portion of the ZOA performed.

3. Cell filled with mercury and ZOA completed.

Individual measurements were made using the following sequence of steps:

33

a. Cell was disconnected, emptied, rinsed with pure water and reconnected to the LCR meter,

b. Open circuit portion of ZOA performed,

c. Cell filled with sample,

d. Temperature of sample measured.

e. Test solution description and temperature entered into the HP-85 computer,

f. The measurement program was run.

This procedure was devised using cell #1. As cell #2 had a drain port, draining and rinsing the cell was accomplished without disconnection of the cell. Therefore cell #2 runs followed the same procedure except for disconnecting the cell and performing the open circuit portion of the ZOA.

The measurement program provided the specific instructions to the LCR meter. The program was written using the LCR meter and computer operating manuals [Ref. 15 and 18] and followed suggested sample programs. Initially, the program defined the instrument circuit mode, test signal level, measurement range and trigger source. A repetitive measurement sequence followed. At each test frequency the impedance (magnitude and phase), inductance, resistance, voltage, and current were each measured 100 times, averaged, and recorded. This constituted one measurement run and was repeated for each new sample.

C. SAMPLE PREPARATION

Solutions of magnesium sulfate, sodium chloride, potassium bromide, and potassium chloride were prepared

from pure solid chemical. Since magnesium sulfate is deliquesent, the procedure for preparation of solutions of the proper salinity was somewhat complex. Mallinkrodt Analytical Reagent Anhydrous magnesium sulfate was placed in a clean dry pyrex beaker and heated in an electric furnace at 130C for several hours after which the powder was placed in a Scheibler lime glass desiccator and allowed to cool to room temperature. Stock solutions ranging from a salinity (denoted S) of .1 to 100 were desired. Salinity is defined as: 100 (wt of solute) / (wt of solution). Preparation of the specific solutions was done by estimating the volume of solute needed, obtaining that amount from the desiccator and rapidly weighing the solute plus polystyrene balance pan. All weighings were done on a Sartorius analytical balance type 2403 accurate to .0001 grams. Several practice weighings were done in this manner, and the rate of water vapor absorption by the magnessium sulfate was estimated. Using these figures, the sample weights were assigned the accuracy of .001 grams. Once weighed, the magnesium sulfate was transfered to a clean dry volmetric flask. Pure water was added to the flask using a 50 ml precision burette until the solution volume was 250+/-.12ml (as indicated by the calibration line on flask). The weight of solute and water used were recorded.

Mallinckrodt U.S.P. grade sodium chloride, Mallinckrodt analytical reagent grade potassium chloride and Fisher

35

certified research grade potassium bromide were used to prepare the stock solutions of each specific reagent. Solution preparation was similar to that for magnesium sulfate; except that the heating and rapid weighing necessitated by the hygroscopic nature of the magnesium sulfate was not required for the other reagents.

D. EXPERIMENTAL RESULTS

The experimental data is divided into 3 sections; background measurements, cell #1 data and cell #2 data.

Prior to the data runs, the ZOA was performed as described earlier. After the ZOA, the response of the measurement system was recorded for two specific samples; pure water and mercury. These results are presented in Appendix A, and were used in the following section to analyse the data.

Thirty-two samples were measured using cell #1 and the data is presented in Appendix B in tabular form. Select data sets characteristic of the rest are presented in graphical form. Potassium chloride was chosen as representative, and the results for salinities of 1, 25 and 100 are shown in Figures 6, 7, and 8 respectively. Presented in these figures are the raw data points and for comparison, the response of the experimental model (solid line). Potassium bromide, sodium chloride and magnesium sulfate at a salinity of 25 are also shown in Figures 9, 10, and 11 respectively.

36
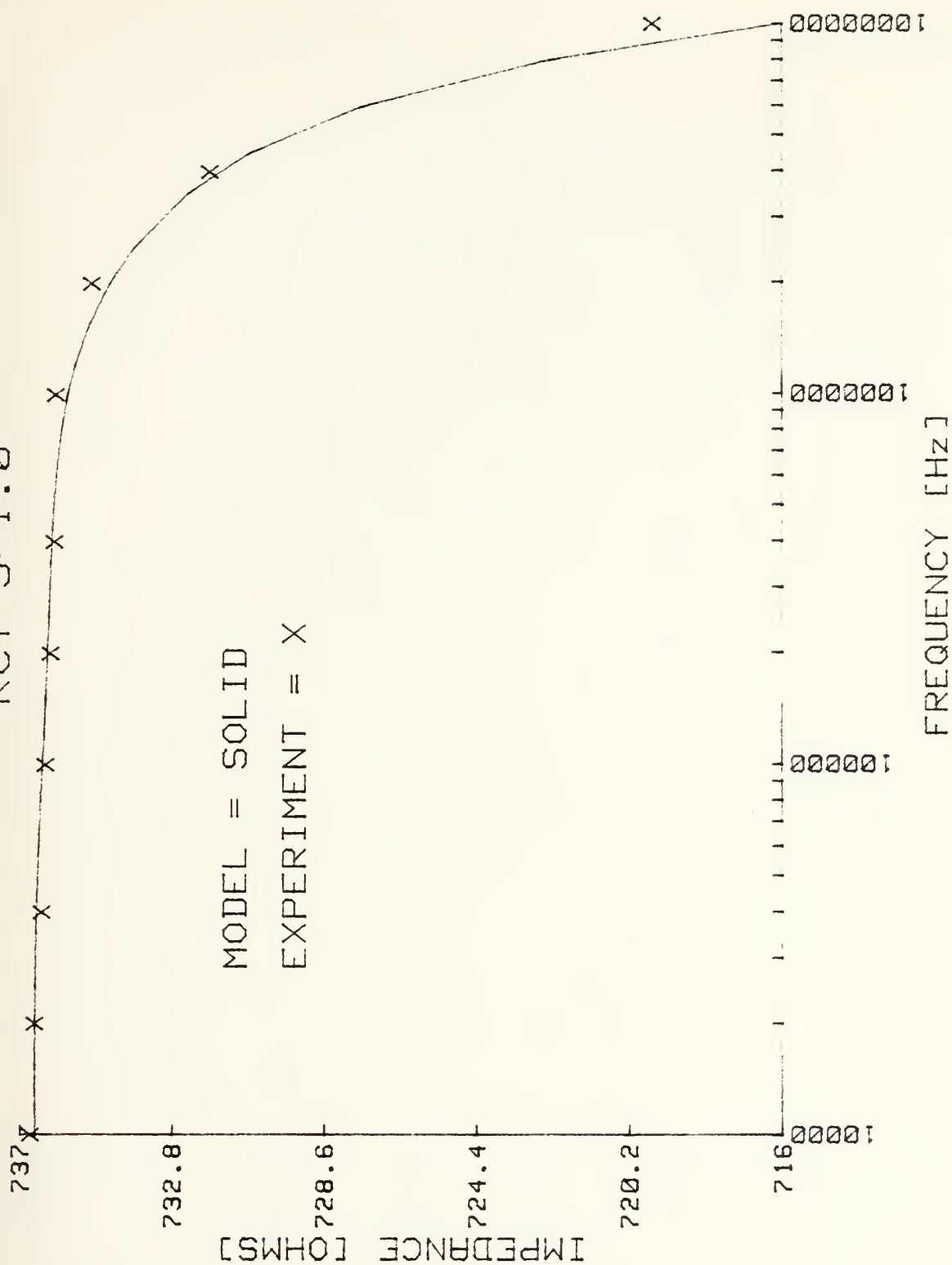
Figure 6.   Impedance vs. Frequency for KC1 S=1.0
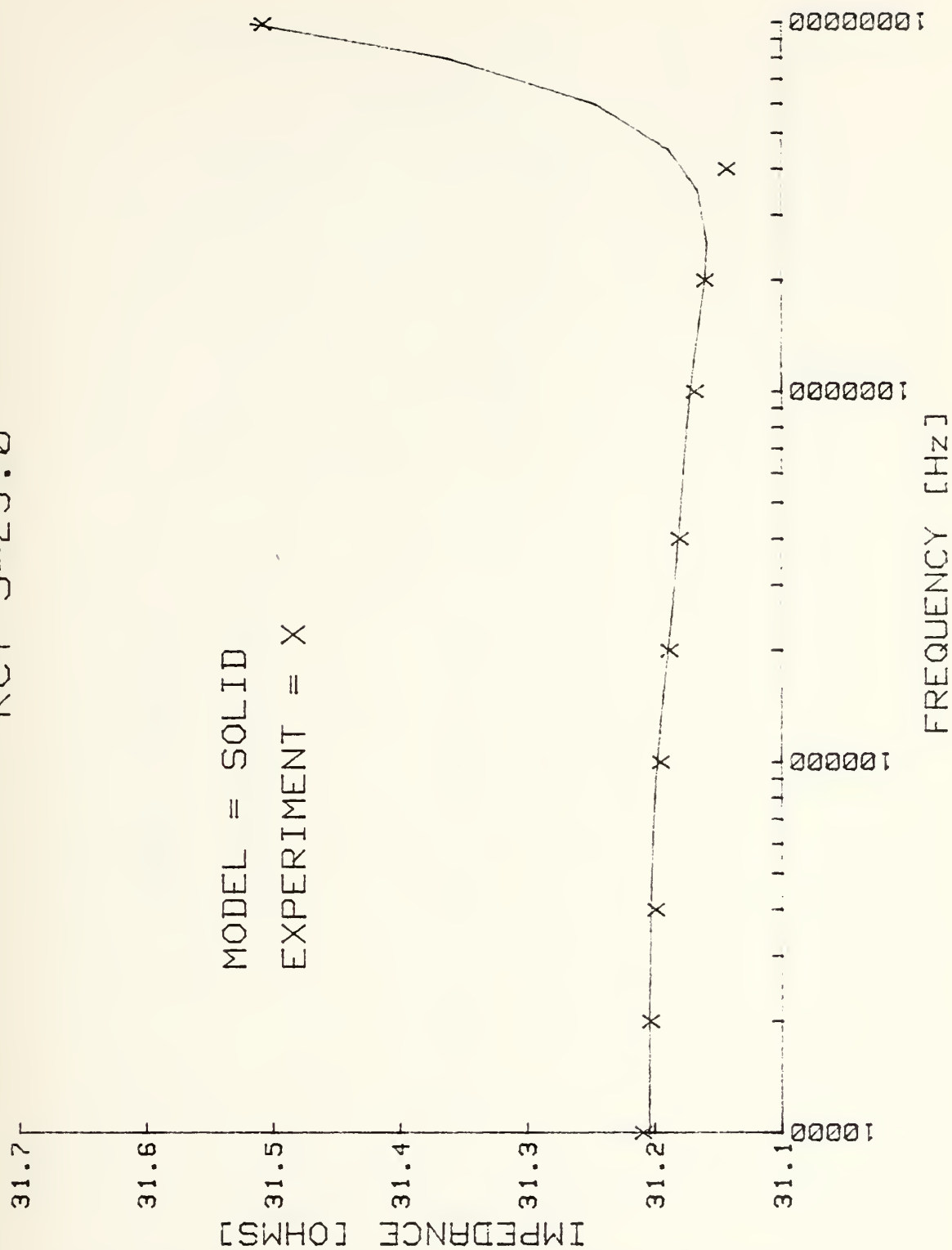
37

Figure 7.   Impendance vs. Frequency for KCl S=25

38
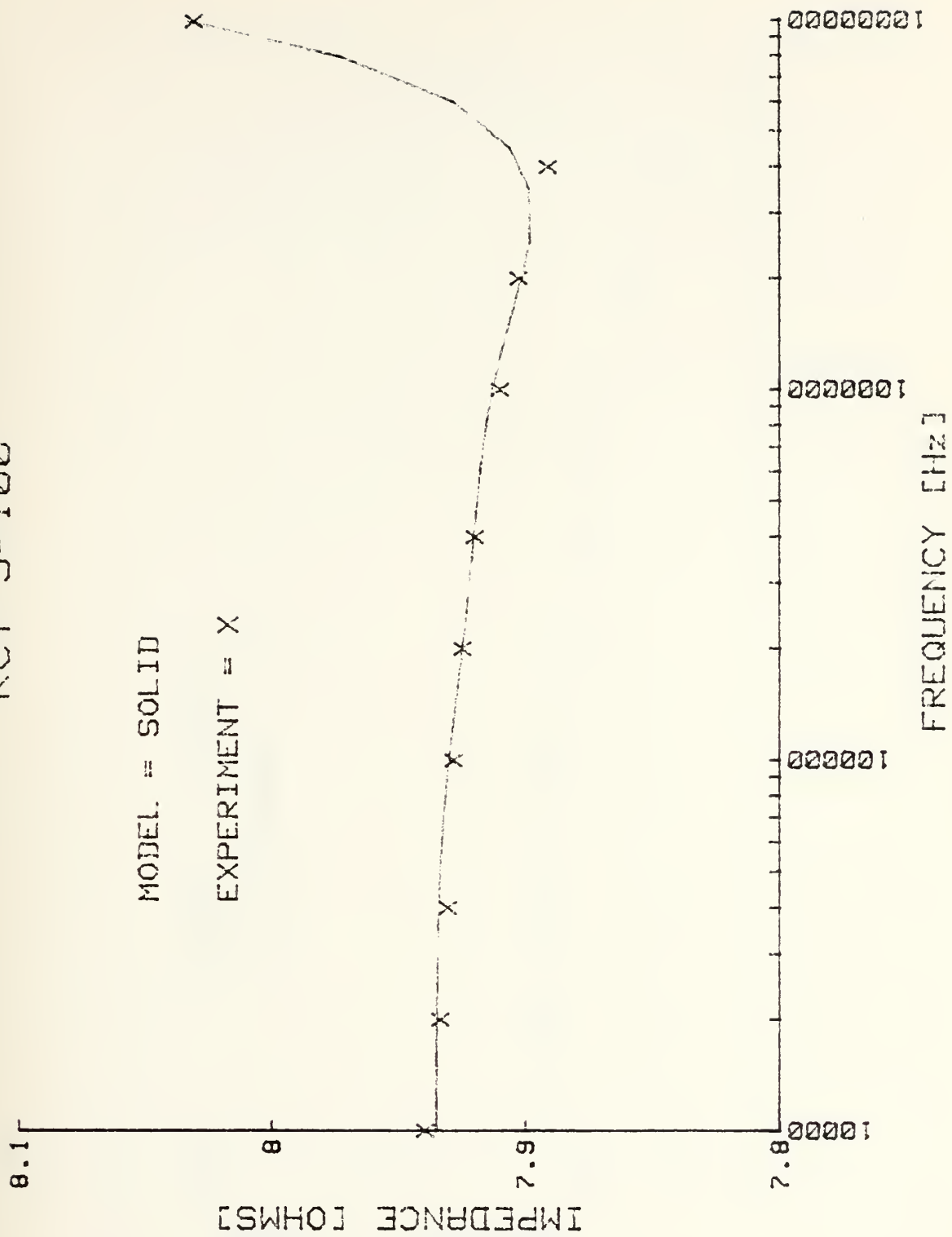
Figure 8.   Impedance vs . Frequency for KCl S=100

39
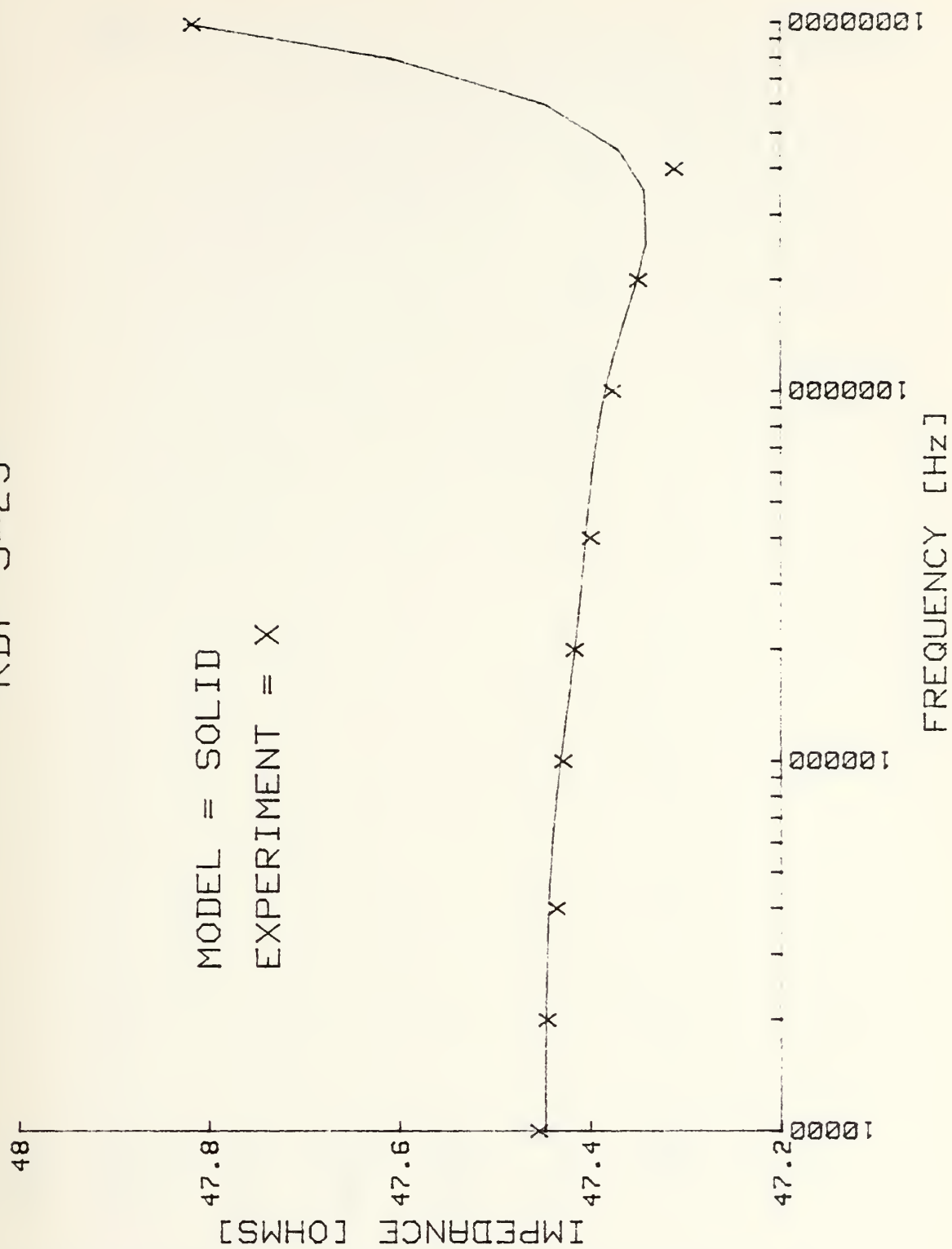
Figure 9. Impedance vs. Frequency for KBR S=25

40
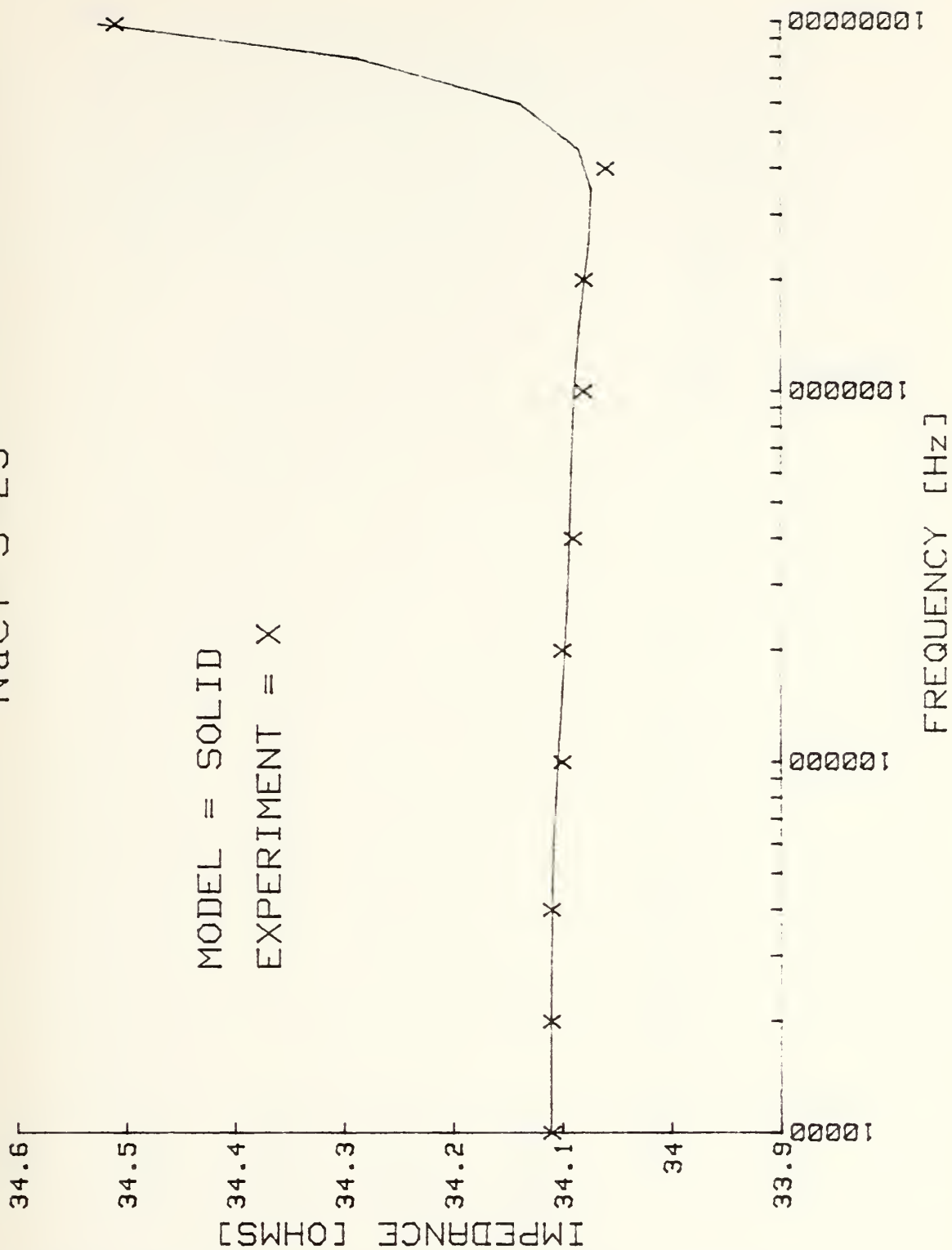
Figure 10.   Impedance vs. Frequency for NaCl S=25

41
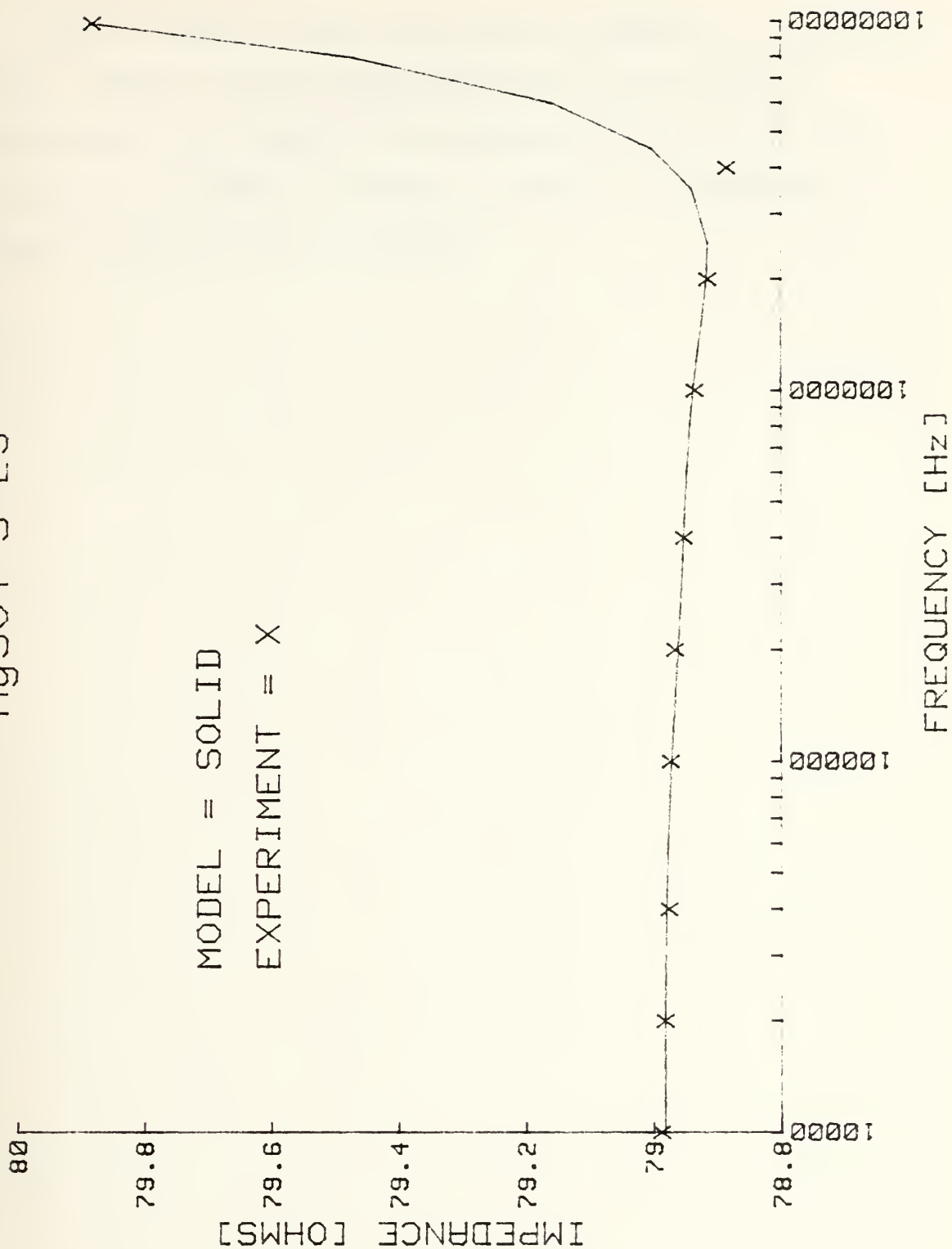
Figure 11.   Impedance vs. Frequency for MgSO4 S=25

42

Cell #2 data is also presented in Appendix C in tabular form. Sodium chloride and magnesium sulfate data at salinities of 25 and 100 characterized the data and are presented in Figure 12 through Figure 15 in graphical format similar to cell #1 data.
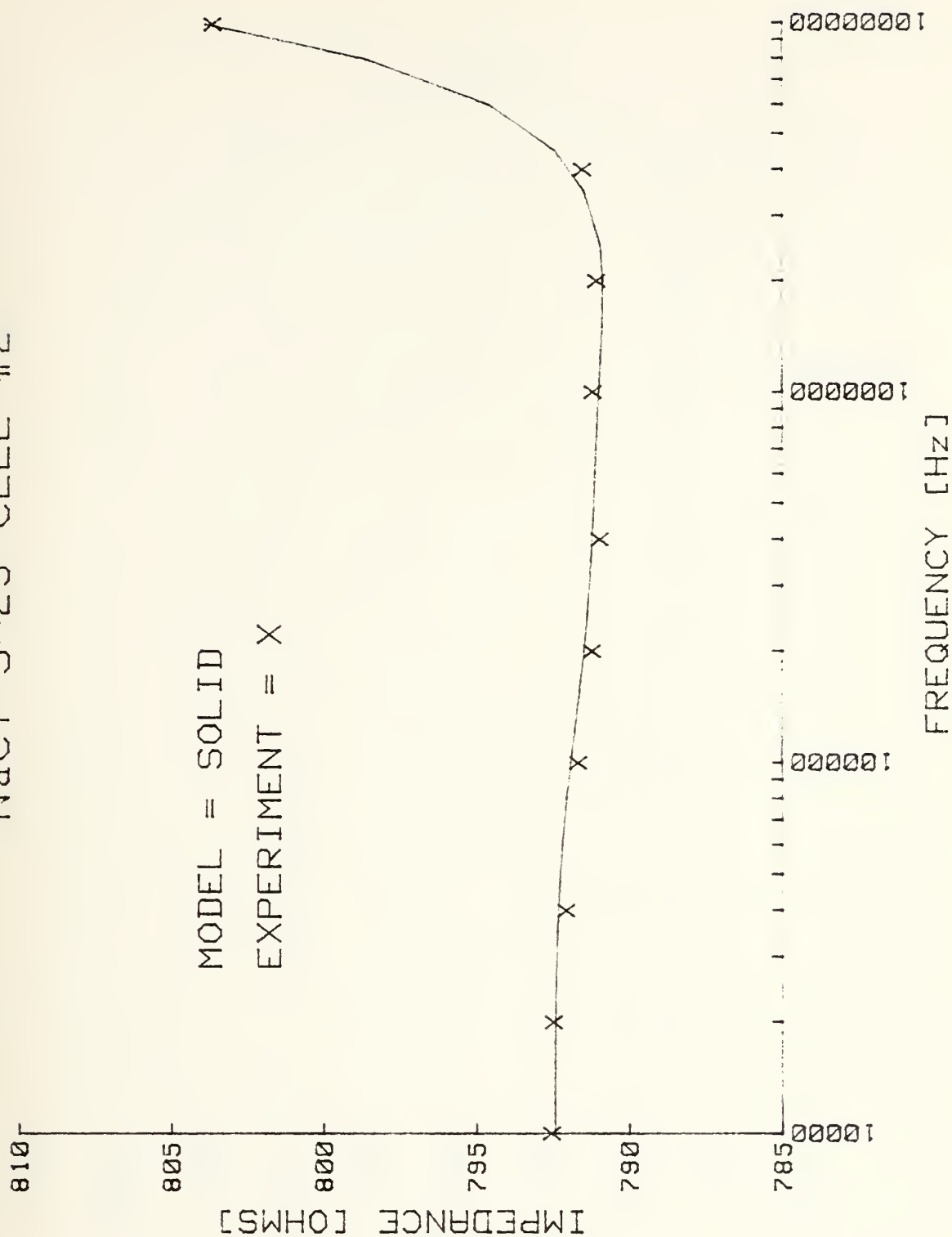
Figure 12. Impedance vs. Frequency for NaCl Cell #2

44
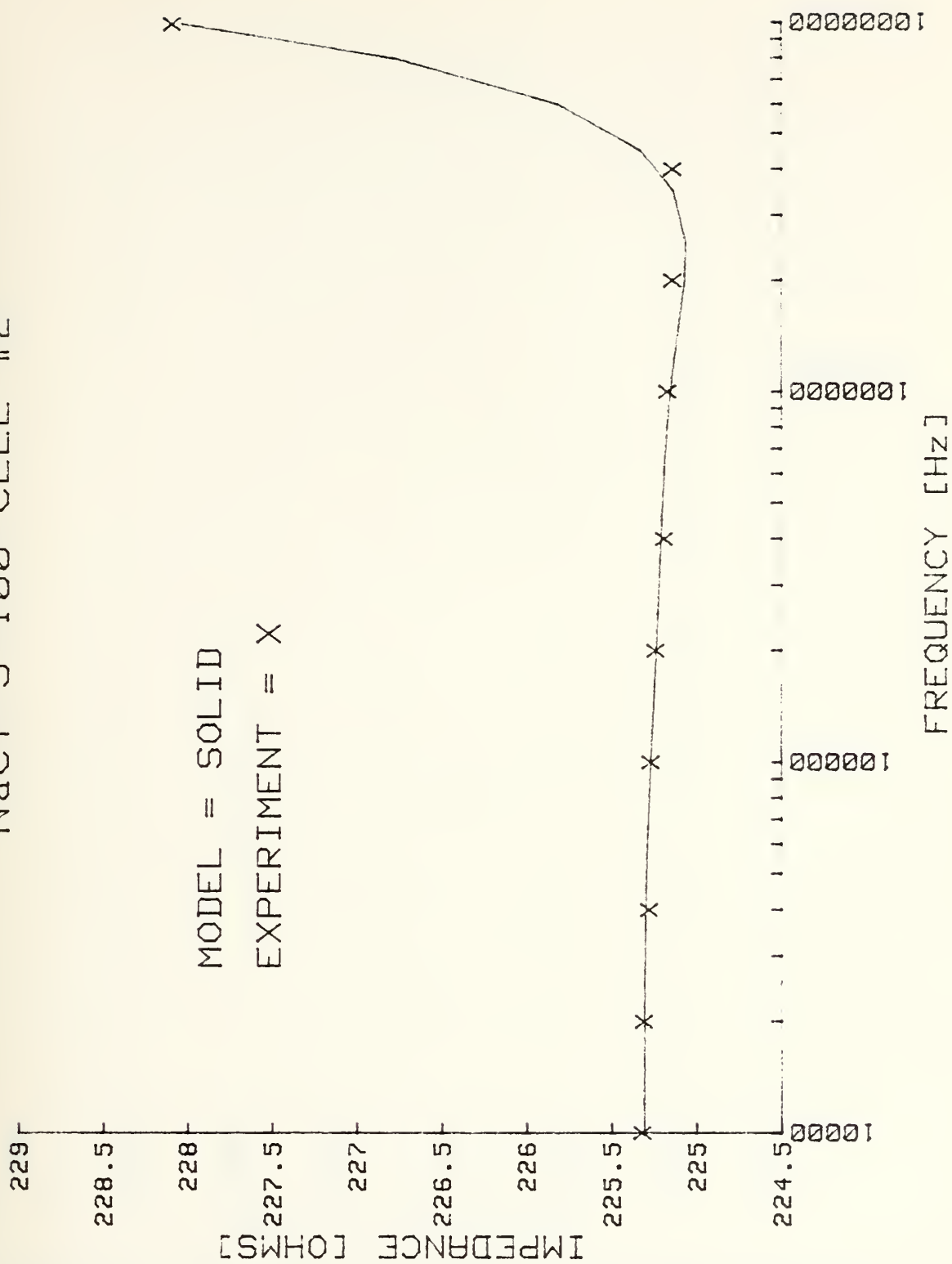
Figure 13.   Impedance vs. Frequency for NaCl S=100 Cell #2

45
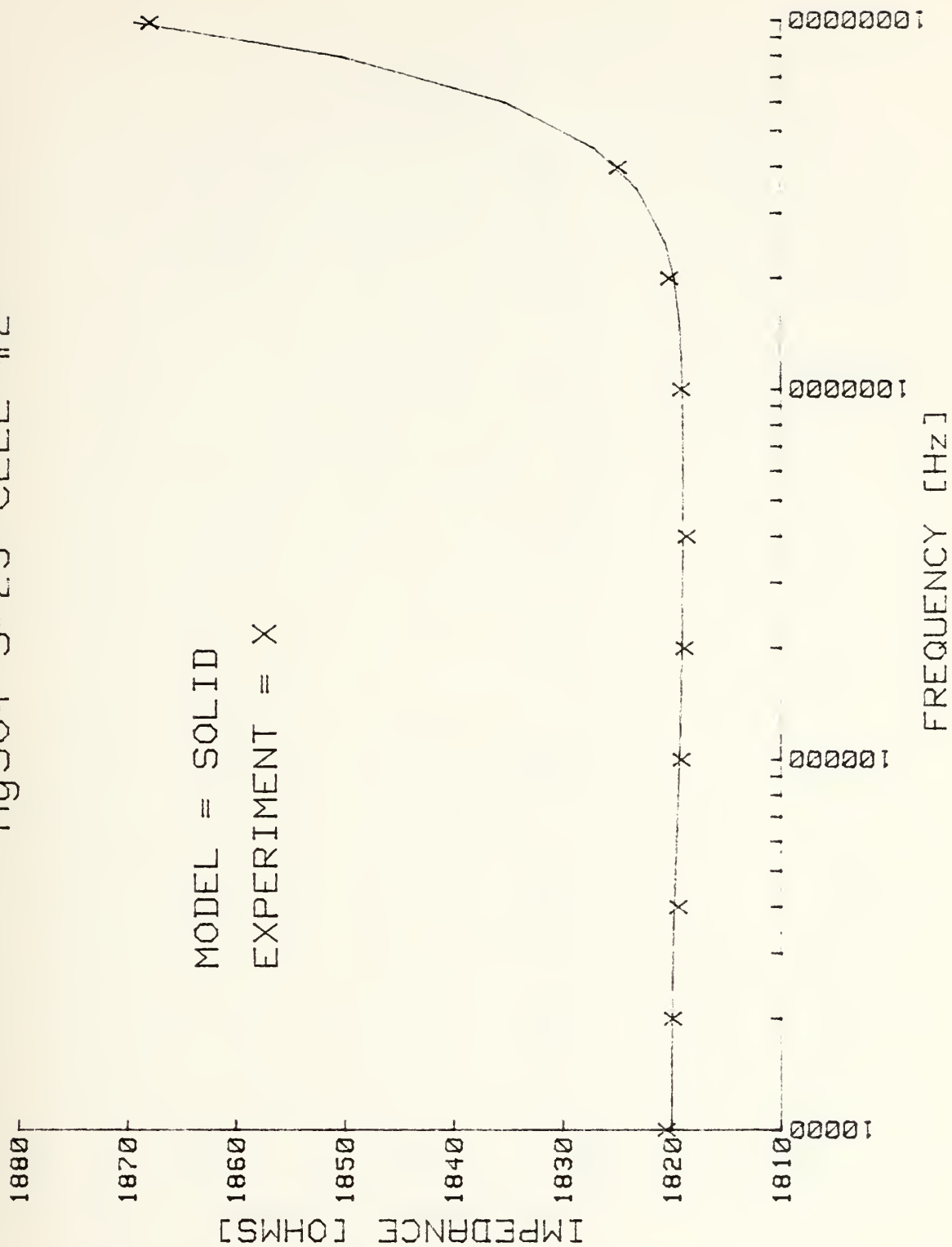
Figure 14. Impedance vs. Frequency for MgSO4 S=25 Cell #2

46
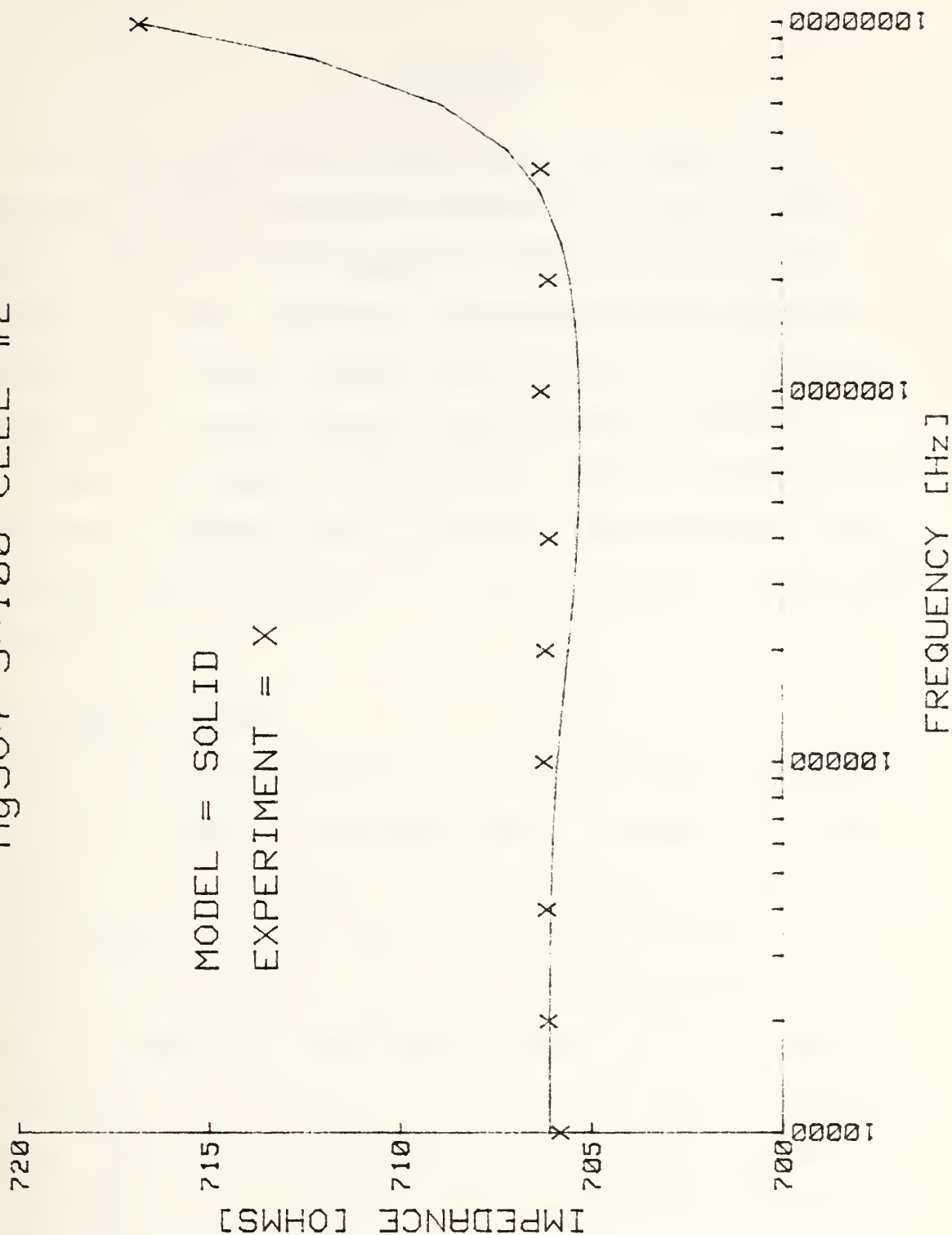
Figure 15. Impedence vs. Frequency for MgSO4 S=100 Cell #2

47

V. ANALYSES

The raw data from the experiment consisted of the
magnitude of the impedance (denoted by Z) and the phase
angle, which were the response of the test fixture and
sample. A simple equivalent electrical circuit has been
derived in section IV that simulated the test fixture and
sample. With this circuit, the raw data was used to
calculate the effect of the sample. Part A describes how
the sample response was calculated. Part B presents this
secondary data, and Part C discusses accuracy and sources
of error.

A. SAMPLE RESPONSE

The equivalent electrical circuit has been derived in
section III, and is presented again in Figure 16b. The
value of C was determined using the response of pure water,
the predominant constituant of the test solution. This
left the six remaining parameters to be determined for
each test solution. The method chosen to do this was
to simplify the equivalent circuit based upon the frequency
range, and generate approximate values for the parameters
after which the magnitude of the impedance was calculated
and compared to the actual data. The model parameters
were then manually changed in an iterative process until
close correlation between calculated and measured data was
achieved.

48

This process was conveniently accomplished using the HP-85 computer and a simple program shown in Appendix D. The frequency range of 10 kHz to 10 MHz was divided into three regions; high, mid and low. Within each region, the raw data was fit to a first degree polynomial (i.e. $f(x) = a + bx$) using the method of least squares [Ref. 19]. The various circuit parameters were obtained from the coefficients of the polynomial. Capacitor C had a very large impedance compared to the rest of the circuit at all frequencies. Since the effect of the capacitor C was small, for it was a large parallel impedance, it was ignored in the simplified circuits.

In the high frequency region, 4 to 10 MHz, the circuit model simplified to that shown in Figure 16b. Capacitors C1 and C2, although different, represented a small impedance and short circuited resistors R1 and R2. The simple series RL circuit remained. The raw data for this region was fitted to the equation $Z^2 = R^2 + (L\omega)^2$ and provided values for R and L.

The mid frequency region, 200 kHz to 2 MHz, has the simplified circut model shown in Figure 16c. The capacitor C was larger than C2 and shorted out resistor R1. The inductor L also represented a small impedance and was ignored. The data was fit to the equation

$$Z^2 = (R + R2)^2 + (\omega C2R2)^2 (R^2 - Z^2)$$

49

(this is linear in ω^2). Using the coefficients of the
polynomial and the previously calculated value of resistor
R, values of C2 and R2 were computed.

The low frequency region, 10 kHz to 100 kHz, circuit
model is shown in Figure 16d. Capacitor C2 was smaller
than C1 and presented a large impedance in this region;
it was largely masked by the resistor R2 and subsequently
ignored. The inductor L represented a small impedance
and was also ignored. The data was fit to the equation

$$Z^2 = (R + R1 + R2)^2 + (\omega C1 R1)^2 ((R + R1)^2 - Z^2)$$

Using the coefficients and previously calculated values
for R and R2, C1 and R1 were calculated.

The program then computed the magnitude of the impedance
based on an analytical form derived from the complete
equivalent circuit model. Using the approximate parameter
values previously obtained, impedance values were calculated
for each frequency and compared to raw data. An iterative
process followed where new values were entered manually for
each parameter to more closely duplicate raw data. The
final set of six parameters represented the best modeling
of the raw data and was recorded along with the comparison
impedance values at each frequency.

B. CALCULATED RESULTS

As developed in section III, the conductivity can be
expressed in terms of the resistance R and inductance L.
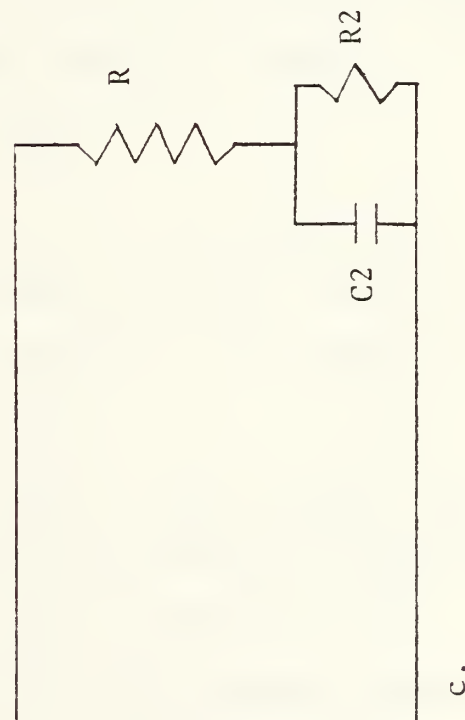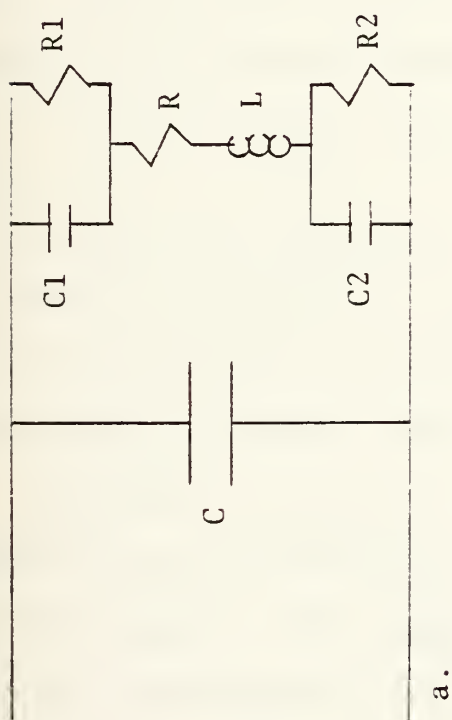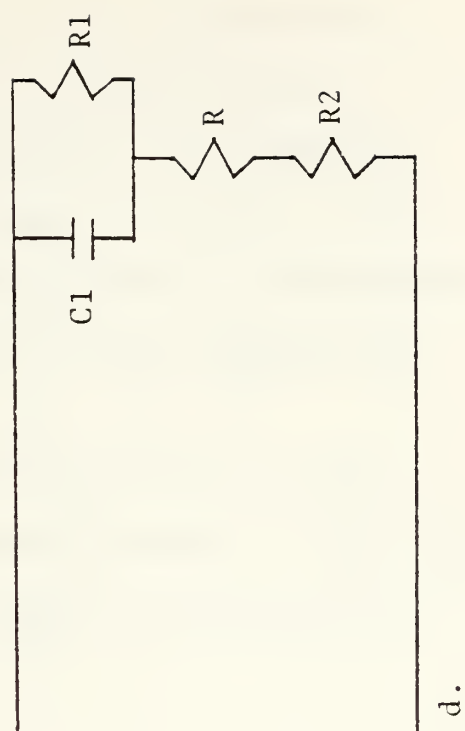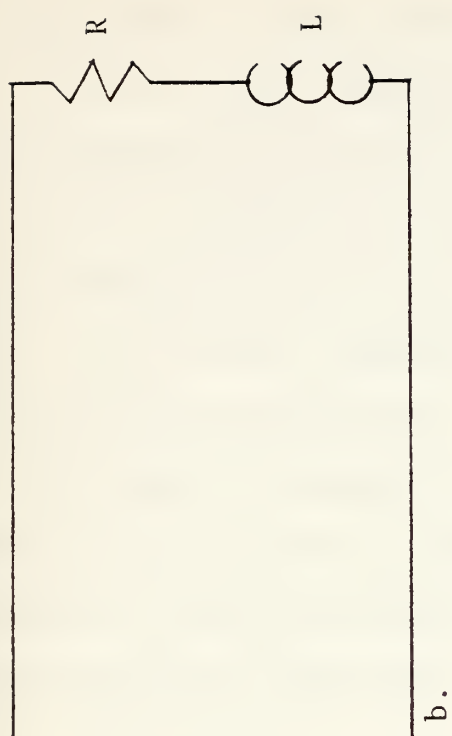
Figure 16. Simplified Model Circuits

51

The real part of the conductivity at low frequencies is
$K_o = k/r$, k = cell constant, and is often referred to in
the literature as the D.C. conductivity. The imaginary
part of the conductivity is $K_o(\omega/b)/(1 + (\omega/b)^2)$, which
can be characterized by the damping factor b, which equals
R/L. The real and imaginary parts of the conductivity
are considered separately.

The damping constant b is the reciprocal of the
conductivity relaxation time (non-dielectric). This inter-
pretation follows from the development in Section III,
specifically the equation:

$$m d<v>/dt + m b<v> = qE.$$

When the applied E-field is turned off, the charge carriers
return to equilibrium and the mean velocity becomes:

$$<v> = <v(t = 0)> \exp(-tb).$$

The conductivity relaxation time, $1/b$, is designated Tc.
A summary of Tc for all cell #1 data and select cell #2
data is presented graphically in Figure 17. Tc data is
also shown in tabular form in Table 1.

Displayed in Figure 17, the general trend of the time
constant was to increase with increased salinity, regardless
of the reagent. This suggested that the effect of the
ion-ion interactions were cumulative; the mobility decreased
as the number of ions increased. Also of note was the
relatively small variation in time constant with either

52

Figure 17. Non-Dielectric Time Constant Comparison

Table 1. Time Constant Data

| | | Tc DATA (ns) CELL #1 | | |
S	MgSO4	KCl	KBr	NaCl
.1	.516	.784	.09	2.64
1	.265	.899	.5636	1.00
4	1.118	1.897	1.527	2.19
10	1.972	2.36	2.12	2.88
25	2.351	2.511	2.31	3.33
49	2.481	2.416	2.254	3.44
64	3.04	1.928	2.49	3.298
100	3.14	3.31	2.18	4.25

CELL #2

S	MgSO4	NaCl
25	3.64	2.98
100	2.99	2.83

54

salinity or reagent. A change in salinity by 100 resulted
in a change in time constant by less than 10. The variation
of Tc with S showed definite structure unique for each
reagent. Analysis of this structure would require a more
sophisticated theoretical model, and was not pursued further.
As discussed in part C, accurate results for salinities
less than one were fundamentally more difficult to obtain
due to cell design. Consequently, they were at best an
approximation to actual sample response and were ignored
in any analysis.

The parameter R related to the real part of the
conductivity, specifically Ko = 1/r per unit length. The
Ko results for this experiment are presented graphically
in Figure 18 and in tabular form in Table 2. Following
Smedley [Ref. 20], Ko was expressed in units of semens/meter
as opposed to one of many possible historical forms.

Early models of the concentration dependance of Ko are
presented by Falkenhagen [Ref. 21] and for low concentrations
are of the form:

$$Ko = S(A - B(S)^{.5})$$

where S is the salinity and A and B are constants. Accordingly,
data points would form straight lines of negative slope if
plotted as Ko/S vs. (s)^.5 as in Figure 19. Calculated
data correlated poorly to this model, as expected, for the
low concentration assumption was no longer valid. Experimental
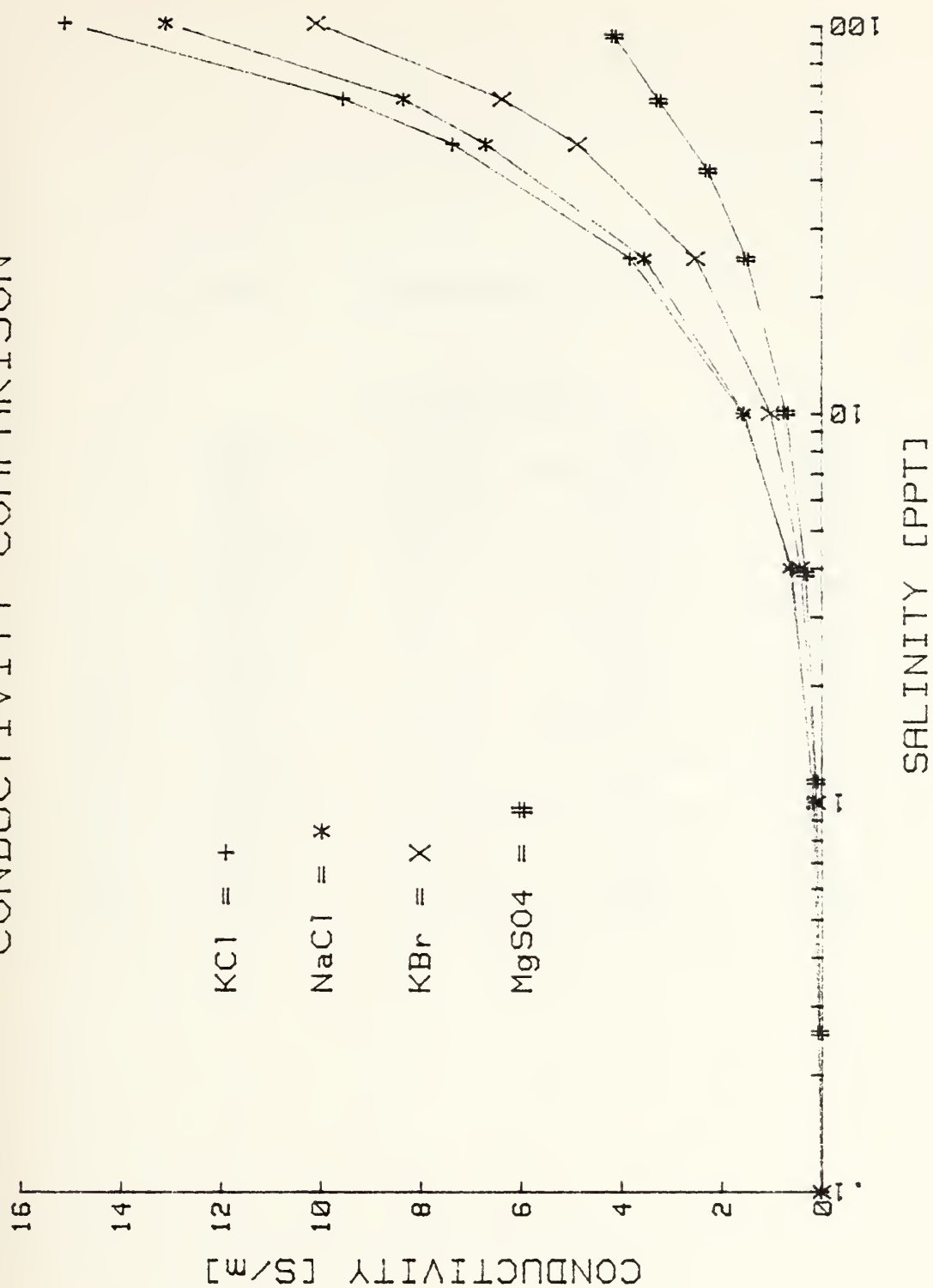
Figure 18.   Conductivity Comparison

56

Table 2. Conductivity Data

Ko DATA (S/m)

S	MgSO4	KCl	KBr	NaCl
.1	.408	.0186	.0119	.0268
1	.1258	.162	.1116	.175
4	.331	.609	.4269	.635
10	.7211	1.583	1.029	1.553
25	1.51	3.825	2.517	3.536
49	2.268	7.361	4.869	6.693
64	3.248	9.542	6.373	8.337
100	4.139	15.115	10.083	13.098
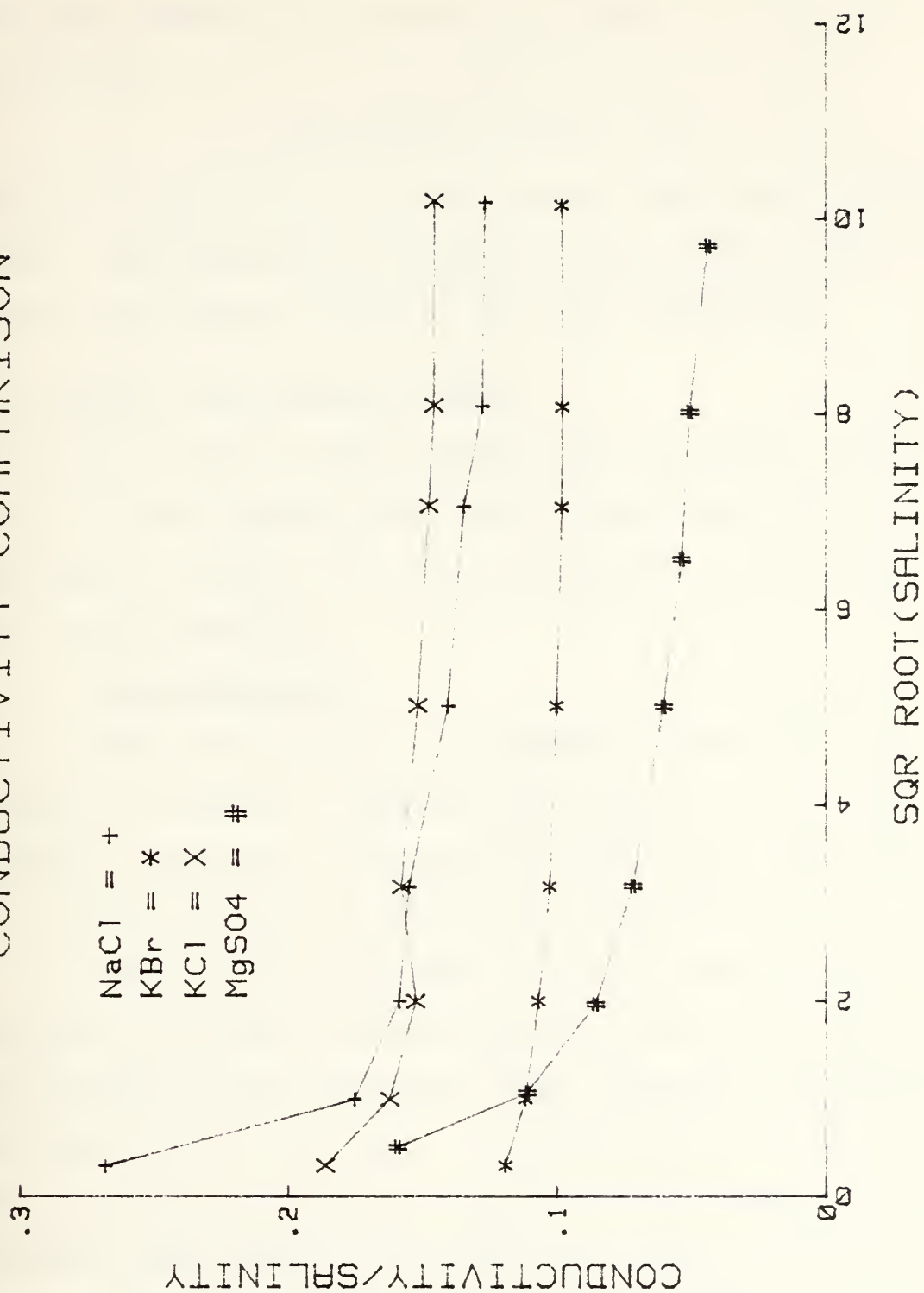
Figure 19.   Conductivity Comparison; Falkenhagen Model

data more closely fit an emperical formula by Walden [Ref. 22] of the form:

$$Ko = SA/(1 + B(S)^{.5})$$

Plotting S/Ko vs. (S) ^.5, data points would form straight lines. Data presented in Figure 20 approximated this linear relationship very well at higher salinities.

C. ACCURACY AND SOURCES OF ERROR

This section has been divided into two parts. Part 1 deals with the accuracy and errors associated with the measurement process while Part 2 discusses the errors in the derived quantities.

1. Measured Values

The data consisted of impedance (magnitude and phase) at a specific frequency for a given solution of reagent. Therefore the overall accuracy was a function of the accuracy of each of these three parameters.

The HP-4275A LCR meter was used to measure the impedance. The meter operating manual [Ref. 23] describes the accuracy of the magnitude of the impedance, designated Z, and phase angle separately. Z accuracy was a function of both the test frequency and the measurement range. High frequency measurements were inherently more difficult to make and were subsequently less accurate. Table 3 presents a summary of the impedance measurement accuracy. The ten test frequencies were preset by the LCR meter with an accuracy of .01%.
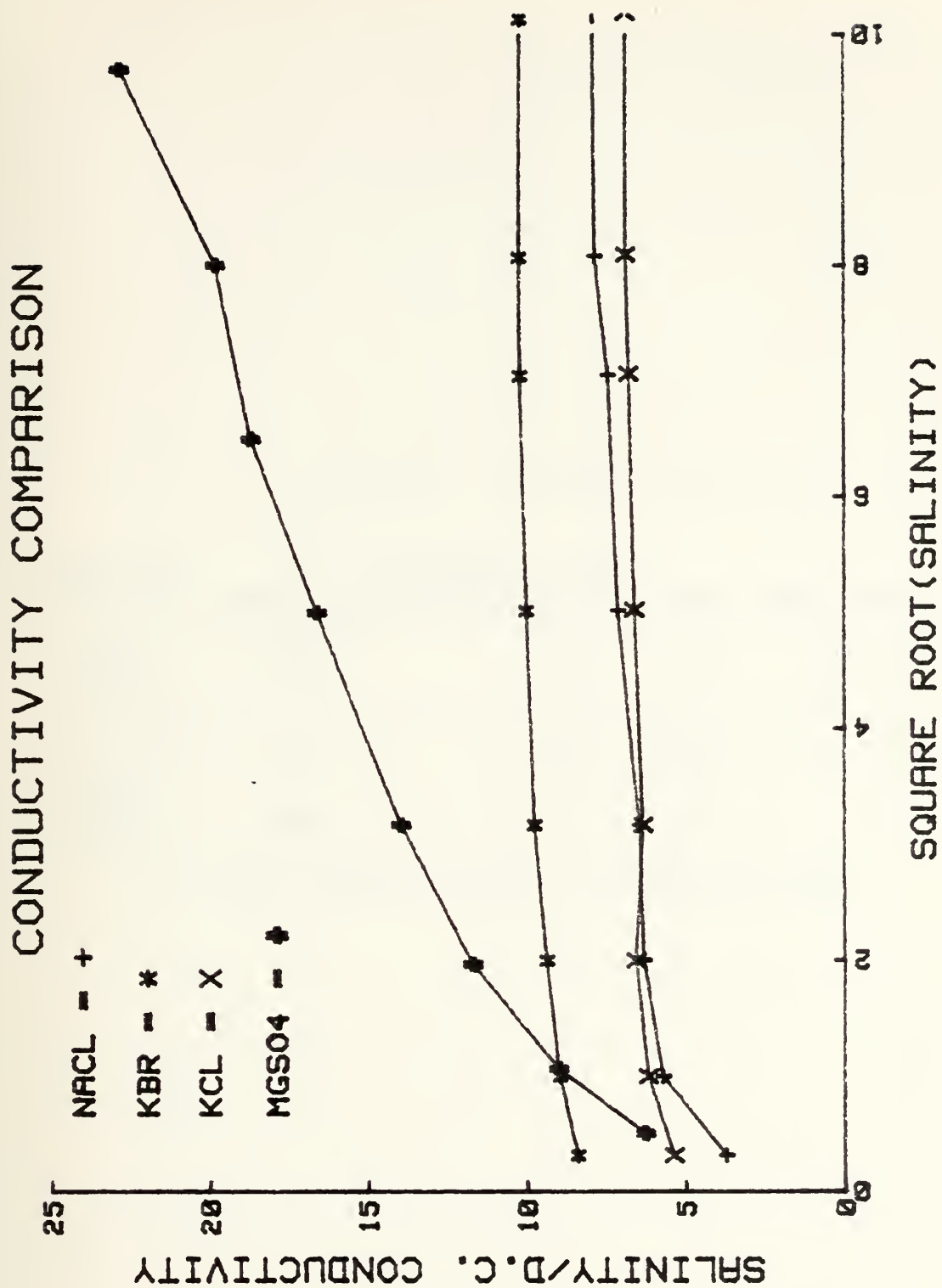
Figure 20. Conductivity Comparison: Walden Model

Table 3. Impedance Accuracy

PARAMETER VALUE	FREQUENCY RANGE			
	10kHz-100kHz	200kHz-1MHz	2MHz	4MHz-10MHz
Z<199 (OHMS)	*.2%	.3%	.7%	2.1%
Z>199	.4%	.5%	1.1%	3.1%
PHASE ANGLE (DEG)	.1	.1	.3	.9

* .2% OF METER READING = POTENTIAL ERROR

Preparation of the samples involved two primary sources of error; the liquid volume and the sample weight. Volume measurements were made using a 50ml precision burette with an accuracy of .1ml for sample concentrations greater than salinity of 4. For lower concentrations, liquid volume was determined using volumetric flasks accurate to .12ml. All sample weights were measured using the Sartorious balance described earlier, accurate to .0001g. Stated salinity value accuracy was determined to be 1% following consideration of the absolute accuracy, the sample preparation procedure and potential changes in the solutions while stored in the laboratory (i.e. evaporation/condensation).

An additional source of error not compensated for by the instrument was the skin effect inductance of the electrolytic solution. Calculation of this effect for an electrolytic solution and mercury are presented in Appendix E. The ZOA was performed using mercury, which from Appendix E had a skin effect inductance of about 2nH. This small inductance became part of the compensation for subsequent readings. But the electrolytic solutions had a skin effect inductance of about 5nH, and the difference between them (about 3nH) was the skin effect inductance error. Although present, the size of this error, when compared to the rest of the equivalent circuit, was very small. The previously stated impedance accuracy values adequately account for this additional error.

2. Calculated Data

The accuracy of the calculated results was a function of the accuracy of the raw data, the numerical manipulation of the raw data, and the accuracy of the cell constant.

The determination of sample response has been described earlier. A first degree polynomial was fit to the raw data using the method of least squares. From the coefficients of the polynomial vales for all six parameters in the equivalent circuit were calculated. As discussed in Hornbeck [Ref. 24], the method of least squares inherently results in a poorly conditioned coefficient matrix with overall numerical accuracy dependent upon the degree of polynomial used and the number of significant digits of the computing device. Restriction to a first degree polynomial in combination with the 12 digit precision of the HP-85 [Ref. 25] ensured a negligible calculation error in the computed parameter values.

The final set of parameters were determined via an iterative process of comparing calculated impedance magnitude, Z, to raw data at each frequency. The accuracy of this process was dependent upon the optimization criteria and the sensitivity of the calculated Z values to changes in any one of the parameters. Optimization consisted of keeping the difference between calculated and measured data to less than 1% (of the experimental value) at all frequencies. The sensitivity of the calculated Z values

63

to variations in the parameters is shown in Figure 21. MgSO4 at S=25 was chosen as a typical analysis case. Parameters were varied as described from the final parameter set, and Z values recalculated for comparison. The values of R and L were directly related to the test sample while the other four parameters were necessary to describe the test fixture. Comparison with the other parameters showed that the impedance associated with R was much larger than the others. Therefore the calculated Z values were very sensitive to changes in R. The value of L was calculated from data at the higher frequencies, for this was the only region where the impedance associated with L was significant. Consequently, the calculated Z values were sensitive to variations in L at the higher frequencies. Thus the values of R and L served to define the correlation between calculated and observed data, and are not present in Figure 21.

Phase angle raw data was not used in generating the system parameters directly. For most samples, measured phase angle values started at near zero at low frequency and changed only a few degrees. The small phase angle was due to the real part being much larger than the imaginary part of the impedance. The small change in phase angle reflected the small change in impedance of the inductor as frequency increased. Thus the phase angle was insensitive to changes in R and L. Additionally, the measurement error associated with phase angle (Table 3)

Figure 21. Model Sensitivity to Parameter Variation

65

was proportionally much larger than for impedance magnitude. Therefore the small changes in the phase angle had incorporated in them a sizeable error. Early analysis efforts utilizing phase angle comparison were discontinued due to large variations in output parameters. The sensitivity and inherent error associated with phase angle data relegated its immediate usefulness to that of an indicator of data trends only.

For samples of salinity less than one, an additional complication occurred. When considering the equivalent electrical circuit, the parameter C was ignored in the preliminary analysis for it was a large impedance relative to the rest of the circuit. For low salinity samples, this relationship was not as valid; the resisitance R of the sample was much larger and approached the impedance of C within an order of magnitude. Thus the raw data reflected the response of C partially masking the response due to R and L. As a consequence, the subsequent processing of raw data to determine values of R and L was more difficult. Calculated impedance was much less sensitive to variations in L and R. Accordingly, stated parameter values were approximations of sample response and useful as indicators of data trends for this low salinity region.

The cell constant for cell #1 was determined to be 1.188 +/- .0012 1/cm using the data and procedure in

Harned and Owen [Ref. 26] in conjunction with the LKB
conductivity bridge. The conductivity bridge was calibrated
18 March 1983 and certified accurate to .1%. Several
resistance measurements were made and the mean value used
in computing the cell constant.

VI. SUMMARY AND RECOMMENDATIONS

The central result of this experiment was the determination
of the electrolytic conductivity as shown in Tables 1 and 2.
The experiment was designed to use direct measurements
of the impedance and included development of a model for
the electrical characteristics of the complete test fixture
system and a theoretical model for the conductivity.
Isolation of the sample response from the overall test
fixture response was accomplished using the system model.
The conductivity model enabled interpretation of the sample
response and subsequent calculation of the electrolytic
conductivity of the sample.

The physical measurement of the electrolytic conductivity
was sensitive to the temperature, solution concentration and
especially design limitations inherent in both the test
fixture and measurement system. Emphasis of the imaginary
part of the conductivity (i.e. the inductance L) occurred
near 10 MHz. The combination of only preselected test
frequencies, an upper frequency limit of 10 MHz on the measure-
ment instrument, and a frequency dependent absolute measurement
error that dominated the overall accuracy around 10 MHz
resulted in relatively few data points for analysis and
made accurate determination of the inductance L more difficult.
Additionally, the measured impedance of low concentration
samples was dominated by the capacitive character of the

test cell. This largely masked the response of the sample
and further complicated determination of the sample
paramters.

The observed changes in impedance were often small
making precise quantitative comparison with theory difficult.
However, certain qualitative conclusions are evident:

1. The experiment has demonstrated correlation between
measured data and a conductivity model which accounts for
the inertia of the charge carrier to within 1%. The
absolute measurement error (see Table 3) increased with
frequency, with the largest error less than 3.5%. The
conductivity of the test solutions decreased with increased
frequency.

2. The first measurements of the non-dielectric time
constant, Tc, defined by the conductivity model, were
generally of the order of nanoseconds. Tc was relatively
insensitive to reagent type and concentration and changed
by a factor of 10 for salinity changes of 100.

3. Observed trends in the D.C. or real part of the
conductivity followed the empirical formula introduced
by Walden in 1906 which characterizes similar data from
other research.

The proposed conductivity model has been shown valid
in the frequency region between 10 kHz and 10 MHz, and
provides a macroscopic rather than a microscopic description
of the actual chemical processes involved.

Future research is necessary to provide precise numerical values and to supplement a more sophisticated theoretical model. This work directly invites a number of follow-on investigations of phenomena associated with:

- the temperature dependence of the conductivity, which is important both for a general understanding of the electrolytic conductivity and in specific areas such as biological systems

- the concentration dependence of the conductivity, in the low concentration regime utilizing more sensitive test cells which would provide more information on the microscopic nature of charge transport in solutions

- attenuation studies utilizing actual signal attentuation rather than measured impedance variation to further verify conductivity theory by independent measurements

- conductivity experiments using complex solutions formed by combining multiple reagents and a solvent which more closely simulate practical electrolytic systems and provide data to extend theoretical models of solutions.

 All of which are important and ultimately necessary to correctly determine the conductivity of seawater.

APPENDIX A

BACKGROUND DATA

CELL #1 DATA

| Hz | pF | POST ZOA | | | POST RECONNECTION | | |
		OHMS	DEG	nH	OHMS	DEG	nH
1E+04	6.9126	.00138	0	4.600	.00265	0	5.000
2E+04	6.8048	.00152	0	1.600	.00272	0	1.800
4E+04	6.6828	.00160	0	0.000	.00275	0	0.000
1E+05	6.5344	.00172	0	.280	.00282	0	.520
2E+05	6.4078	.00181	0	.100	.00286	0	.240
4E+05	6.3089	.00193	0	.400	.00288	0	.220
1E+06	6.2212	.00211	0	.092	.00302	0	.192
2E+06	6.1658	.00226	0	.016	.00406	0	.114
4E+06	6.0827	.00668	0	.016	.00996	0	.048
1E+07	5.9163	.06258	0	1.131	.08746	0	1.702

CELL #2 DATA

| Hz | pF | POST ZOA | | | POST RECONNECTION | | |
		OHMS	DEG	nH	OHMS	DEG	nH
1E+04	.1356	.00080	0	3.800	.00070	0	4.400
2E+04	.1386	.00066	0	1.000	.00058	0	1.600
4E+04	.1437	.00056	0	1.000	.00052	0	0.000
1E+05	.1538	.00052	0	.040	.00058	0	.640
2E+05	.1692	.00078	0	.160	.00090	0	.500
4E+05	.1951	.00140	0	.700	.00138	0	.020
1E+06	.1913	.00320	0	.228	.00378	0	.476
2E+06	.1724	.00580	0	.306	.00570	0	.410
4E+06	.1441	.02094	0	.344	.02298	0	.444
1E+07	.1247	.02290	0	.435	.05138	0	.823

CELL #1 DATA

MgSO4 DATA

Hz	S=.1 OHMS	DEG	S=1 OHMS	DEG	S=4 OHMS	DEG
1E+04	3174.080	-.082	957.760	.016	361.076	-.004
2E+04	3175.200	-.158	958.020	-.001	360.947	-.003
4E+04	3175.500	-.325	958.000	-.060	360.855	-.024
1E+05	3174.600	-.815	958.050	-.241	360.796	-.092
2E+05	3172.000	-1.592	957.720	-.463	360.695	-.173
4E+05	3164.800	-3.110	957.170	-.938	360.561	-.344
1E+06	3132.200	-7.553	955.390	-2.381	360.373	-.886
2E+06	3042.600	-14.515	950.030	-4.644	359.914	-1.720
4E+06	2782.400	-26.600	936.900	-8.849	358.893	-3.357
1E+07	1991.700	-49.837	895.000	-20.316	359.674	-8.014

Hz	S=10 OHMS	DEG	S=25 OHMS	DEG	S=49 OHMS	DEG
1E+04	165.760	-.020	78.988	-.046	52.643	-.069
2E+04	165.742	-.010	78.982	-.027	52.624	-.040
4E+04	165.716	-.017	78.976	-.021	52.610	-.025
1E+05	165.696	-.047	78.973	-.027	52.599	-.021
2E+05	165.669	-.080	78.966	-.035	52.588	-.018
4E+05	165.625	-.154	78.952	-.054	52.572	-.017
1E+06	165.574	-.405	78.935	-.153	52.555	-.053
2E+06	165.476	-.759	78.915	-.254	52.541	-.054
4E+06	165.296	-1.476	78.885	-.499	52.519	-.101
1E+07	166.995	-3.510	79.882	-1.164	53.178	-.166

HZ	S=64 OHMS	DEG	S=100 OHMS	DEG
1E+04	36.941	-.099	29.013	-.122
2E+04	36.926	-.056	28.997	-.071
4E+04	36.916	-.033	28.986	-.038
1E+05	36.908	-.017	28.977	-.016
2E+05	36.899	-.005	28.968	.004
4E+05	36.886	.011	28.956	.033
1E+06	36.870	.024	28.940	.085
2E+06	36.856	.110	28.927	.234
4E+06	36.830	.238	28.899	.487
1E+07	37.351	.714	29.332	1.356

NaCl DATA

Hz	S=.1 OHMS	DEG	S=1 OHMS	DEG	S=4 OHMS	DEG
1E+04	5962.700	-.143	687.930	.007	188.808	-.010
2E+04	5965.700	-.288	688.710	.002	188.825	-.005
4E+04	5967.500	-.600	689.250	-.040	188.826	-.013
1E+05	5966.500	-1.520	689.710	-.166	188.839	-.045
2E+05	5959.000	-2.992	689.940	-.314	188.833	-.084
4E+05	5927.600	-5.916	690.110	-.634	188.822	-.160
1E+06	5733.600	-14.253	689.960	-1.635	188.808	-.432
2E+06	5229.000	-25.987	688.560	-3.221	188.740	-.822
4E+06	4177.220	-42.348	684.330	-6.282	188.582	-1.622
1E+07	2372.060	-64.385	670.960	-14.872	190.383	-3.872

Hz	S=10 OHMS	DEG	S=25 OHMS	DEG	S=49 OHMS	DEG
1E+04	77.360	-.029	34.111	-.059	17.990	-.103
2E+04	77.341	-.016	34.108	-.032	17.988	-.058
4E+04	77.331	-.014	34.105	-.018	17.987	-.028
1E+05	77.330	-.021	34.104	-.009	17.987	-.003
2E+05	77.325	-.027	34.101	.003	17.985	.023
4E+05	77.313	-.043	34.094	.024	17.981	.077
1E+06	77.304	-.128	34.084	.051	17.972	.210
2E+06	77.297	-.207	34.078	.160	17.968	.503
4E+06	77.280	-.411	34.061	.336	17.957	1.088
1E+07	78.290	-.941	34.513	.892	18.214	2.637

HZ	S=64 OHMS	DEG	S=100 OHMS	DEG
1E+04	14.430	-.123	9.249	-.181
2E+04	14.426	-.065	9.246	-.097
4E+04	14.423	-.031	9.244	-.045
1E+05	14.422	-.001	9.243	.004
2E+05	14.420	.034	9.241	.060
4E+05	14.415	.103	9.237	.169
1E+06	14.407	.286	9.228	.478
2E+06	14.401	.663	9.221	1.074
4E+06	14.390	1.430	9.205	2.313
1E+07	14.588	3.454	9.406	5.630

KC1 DATA

Hz	S=.1 OHMS	DEG	S=1 OHMS	DEG	S=4 OHMS	DEG
1E+04	6387.300	-.122	736.720	.009	195.811	-.010
2E+04	6388.800	-.249	736.580	.003	195.834	-.004
4E+04	6388.200	-.530	736.380	-.035	195.815	-.012
1E+05	6387.200	-1.373	736.260	-.155	195.790	-.042
2E+05	6381.500	-2.733	736.120	-.294	195.740	-.076
4E+05	6358.800	-5.460	736.010	-.602	195.677	-.147
1E+06	6211.100	-13.511	735.970	-1.587	195.628	-.405
2E+06	5756.200	-25.667	734.980	-3.170	195.552	-.777
4E+06	4613.800	-43.782	731.720	-6.303	195.481	-1.561
1E+07	2506.600	-67.297	719.560	-15.399	197.630	-3.898

Hz	S=10 OHMS	DEG	S=25 OHMS	DEG	S=49 OHMS	DEG
1E+04	75.395	-.032	31.209	-.072	16.257	-.126
2E+04	75.370	-.018	31.203	-.040	16.249	-.071
4E+04	75.348	-.014	31.199	-.021	16.243	-.035
1E+05	75.333	-.020	31.195	-.009	16.238	-.004
2E+05	75.313	-.024	31.188	.007	16.231	.029
4E+05	75.287	-.036	31.180	.035	16.222	.094
1E+06	75.263	-.110	31.168	.080	16.209	.258
2E+06	75.242	-.173	31.160	.217	16.199	.603
4E+06	75.226	-.349	31.143	.449	16.187	1.302
1E+07	76.143	-.826	31.508	1.217	16.340	3.221

HZ	S=64 OHMS	DEG	S=100 OHMS	DEG
1E+04	12.529	-.156	7.938	-.237
2E+04	12.522	-.083	7.933	-.127
4E+04	12.517	-.040	7.931	-.060
1E+05	12.512	-.002	7.928	.005
2E+05	12.507	.040	7.925	.075
4E+05	12.499	.121	7.920	.209
1E+06	12.488	.341	7.910	.594
2E+06	12.478	.783	7.903	1.323
4E+06	12.465	1.689	7.891	2.845
1E+07	12.549	4.288	8.031	7.626

KBr DATA

Hz	S=.1 OHMS	DEG	S=1 OHMS	DEG	S=4 OHMS	DEG
1E+04	10226.000	-.256	1078.940	.012	279.827	-.003
2E+04	10231.000	-.523	1080.410	-.010	279.875	-.003
4E+04	10229.700	-1.082	1080.570	-.080	279.885	-.020
1E+05	10207.400	-2.724	1080.460	-.290	279.888	-.073
2E+05	10144.100	-5.287	1079.870	-.540	279.821	-.137
4E+05	9954.900	-10.148	1078.690	-1.064	279.698	-.263
1E+06	9145.100	-22.671	1075.600	-2.602	279.493	-.667
2E+06	7617.700	-38.128	1069.070	-4.992	279.181	-1.250
4E+06	5275.000	-55.950	1054.530	-9.540	278.772	-2.432
1E+07	2551.320	-73.887	1000.110	-22.143	280.825	-5.877

Hz	S=10 OHMS	DEG	S=25 OHMS	DEG	S=49 OHMS	DEG
1E+04	116.035	-.016	47.454	-.040	24.533	-.074
2E+04	116.030	-.009	47.445	-.023	24.527	-.043
4E+04	116.018	-.015	47.435	-.016	24.522	-.023
1E+05	116.010	-.033	47.428	-.015	24.518	-.006
2E+05	115.988	-.053	47.416	-.015	24.512	.013
4E+05	115.952	-.095	47.399	-.012	24.502	.046
1E+06	115.905	-.256	47.376	-.040	24.488	.119
2E+06	115.838	-.449	47.349	-.016	24.474	.315
4E+06	115.761	-.862	47.310	.009	24.449	.675
1E+07	117.055	-2.031	47.817	.177	24.679	1.839

HZ	S=64 OHMS	DEG	S=100 OHMS	DEG
1E+04	18.750	-.094	11.864	-.143
2E+04	18.744	-.053	11.859	-.076
4E+04	18.740	-.027	11.855	-.036
1E+05	18.737	-.002	11.852	.001
2E+05	18.732	.026	11.847	.043
4E+05	18.734	.075	11.841	.130
1E+06	18.713	.198	11.830	.364
2E+06	18.703	.479	11.821	.831
4E+06	18.681	1.003	11.805	1.797
1E+07	18.884	2.619	11.899	4.607

APPENDIX C
CELL #2 DATA AND MODEL PARAMETERS

MgSO4 DATA

Hz	OHMS S=1	DEG	OHMS S=4	DEG	OHMS S=10	DEG
1E+04	22025.100	.015	8143.700	.032	3763.230	.003
2E+04	22039.900	.045	8152.800	.052	3767.920	.016
4E+04	22052.600	.085	8161.400	.062	3771.530	.022
1E+05	22069.700	.204	8170.200	.088	3773.890	.033
2E+05	22093.100	.399	8177.700	.180	3774.870	.074
4E+05	22135.000	.760	8186.400	.325	3775.430	.143
1E+06	22293.800	1.729	8205.200	.686	3777.430	.295
2E+06	22697.000	2.970	8236.300	1.287	3781.080	.581
4E+06	24027.000	4.470	8344.800	2.488	3796.560	1.171
1E+07	29103.000	-1.348	9057.400	4.231	3931.130	2.608

Hz	OHMS S=25	DEG	OHMS S=49	DEG	OHMS S=64	DEG
1E+04	1820.460	-.013	1214.990	.040	902.440	.020
2E+04	1819.930	-.001	1215.060	.050	902.600	.039
4E+04	1819.430	.005	1214.560	.054	902.470	.038
1E+05	1819.080	.016	1214.420	.027	902.520	.018
2E+05	1818.790	.039	1214.060	.071	902.400	.053
4E+05	1818.620	.083	1213.830	.100	902.350	.080
1E+06	1819.100	.168	1214.260	.132	902.720	.104
2E+06	1820.230	.341	1213.780	.222	902.480	.188
4E+06	1824.850	.683	1214.450	.437	902.850	.367
1E+07	1867.900	1.591	1235.270	1.047	916.970	.905

HZ	OHMS S=100	DEG
1E+04	705.810	.005
2E+04	706.110	.027
4E+04	706.160	.027
1E+05	706.230	.013
2E+05	706.190	.043
4E+05	706.100	.069
1E+06	706.300	.090
2E+06	706.110	.174
4E+06	706.300	.341
1E+07	716.840	.830

NaCl DATA

Hz	S=1 OHMS	DEG	S=4 OHMS	DEG	S=10 OHMS	DEG
1E+04	16031.200	.070	4406.140	.007	1903.360	-.015
2E+04	16032.300	.105	4402.310	.019	1901.220	-.002
4E+04	16028.900	.132	4398.240	.021	1899.160	.001
1E+05	16032.700	.171	4393.690	.024	1897.280	.007
2E+05	16033.600	.357	4388.710	.051	1895.470	.020
4E+05	16041.000	.639	4384.140	.097	1893.820	.045
1E+06	16101.300	1.376	4381.230	.178	1892.770	.075
2E+06	16257.000	2.531	4379.220	.350	1892.180	.162
4E+06	16852.900	4.496	4388.040	.728	1894.660	.330
1E+07	19927.000	3.670	4512.610	1.604	1931.610	.756

Hz	S=25 OHMS	DEG	S=49 OHMS	DEG	S=64 OHMS	DEG
1E+04	792.540	.005	424.212	-.026	329.090	-.038
2E+04	792.470	.028	423.807	.001	329.120	-.010
4E+04	792.060	.027	423.383	.006	329.085	-.002
1E+05	791.670	.011	423.042	.001	329.098	-.001
2E+05	791.210	.042	422.634	.022	329.056	.015
4E+05	790.960	.067	422.279	.042	329.031	.033
1E+06	791.180	.085	422.043	.050	329.061	.040
2E+06	791.070	.160	421.737	.117	329.050	.100
4E+06	791.520	.312	421.618	.226	329.148	.190
1E+07	803.630	.753	427.338	.508	333.698	.406

HZ	S=100 OHMS	DEG
1E+04	225.323	-.061
2E+04	225.303	-.027
4E+04	225.282	-.012
1E+05	225.272	-.006
2E+05	225.239	.009
4E+05	225.192	.027
1E+06	225.174	.036
2E+06	225.141	.103
4E+06	225.140	.195
1E+07	228.089	.419

77

CELL #1 DATA

NaCl PARAMETERS

S	C1	R1	R	L	C2	R2
S/M	F	OHMS	OHMS	H	F	OHMS
.10	.003	83.600	4438.600	11.7000	.0001	144.370
1.00	.010	2.500	679.000	.6800	.0035	8.000
4.01	.030	1.220	187.000	.4100	.0350	.600
10.03	43.000	.033	76.500	.2200	.0300	.812
25.21	65.900	.019	33.600	.1120	.0480	.492
49.81	100.000	.007	17.750	.0610	.1300	.231
65.40	60.000	.010	14.250	.0470	.1800	.166
103.54	120.000	.009	9.070	.0385	.2100	.168

MgSO4 PARAMETERS

S	C1	R1	R	L	C2	R2
S/M	F	OHMS	OHMS	H	F	OHMS
.26	.045	6.000	2908.600	1.5000	.0001	260.900
1.13	2.500	.375	944.600	.2500	.0048	13.080
3.87	6.000	.355	358.600	.4010	.0300	2.020
10.06	14.000	.101	164.750	.3250	.0510	.880
25.08	40.000	.030	78.690	.1850	.2000	.262
42.38	36.000	.053	52.390	.1300	.3000	.184
64.33	28.000	.064	36.580	.1112	.1420	.292
94.55	20.000	.047	28.700	.0900	.1600	.250

KCl PARAMETERS

S	C1	R1	R	L	C2	R2
S/M	F	OHMS	OHMS	H	F	OHMS
.10	.100	1.000	6378.000	5.0000	.0500	16.300
1.00	4.000	.450	734.000	.6600	.0300	2.140
4.00	8.000	.124	195.060	.3700	.0990	.638
10.04	25.000	.080	75.040	.1770	.2500	.265
25.26	50.000	.026	31.060	.0780	.4500	.121
49.93	55.000	.033	16.140	.0390	.8500	.084
65.60	70.000	.023	12.450	.0240	1.6000	.050
103.97	75.000	.015	7.860	.0260	1.1000	.060

CELL #1 DATA

KBr PARAMETERS

S	C1	R1	R	L	C2	R2
S/m	F	OHMS	OHMS	H	F	OHMS
.10	.500	1.240	10000.000	.9000	.0020	231.000
1.00	.200	.890	1064.500	.6000	.0100	14.680
4.01	3.000	.133	278.300	.4250	.0650	1.430
10.04	11.000	.064	115.500	.2450	.1700	.465
25.19	29.000	.043	47.200	.1090	.3000	.204
49.69	53.000	.024	24.400	.0550	.5500	.105
65.20	60.000	.015	18.640	.0465	.8500	.090
102.93	50.000	.017	11.780	.0257	1.2500	.062

CELL #2 DATA

NaCl PARAMETERS

S	C1	R1	R	L	C2	R2
S/m	F	OHMS	OHMS	H	F	OHMS
25.21	1.000	1.310	789.000	2.3500	.0300	2.120
103.54	13.000	.098	224.400	.6350	.0700	.809

MgSO4 PARAMETERS

S	C1	R1	R	L	C2	R2
S/m	F	OHMS	OHMS	H	F	OHMS
25.08	2.000	1.160	1815.200	6.6000	.0150	3.690
94.55	1.000	.900	703.000	2.1000	.0100	2.190

```
10 OPTION BASE 1
20 DIM F(10),Z(10),T(4),C(10)
30 DISP "ENTER DATA FILE,LABEL
   FILE NAMES"
40 INPUT P$,Q$
50 ASSIGN# 1 TO P$
60 ASSIGN# 3 TO Q$
70 DISP "WHICH DATA COLUMN 1-4"
80 INPUT B
90 READ# 3,B ; L$
100 FOR I=1 TO 10
110 READ# 1,I ; F(I),T(1),T(2),T
    (3),T(4)
120 Z(I)=T(B)
130 NEXT I
140 ASSIGN# 1 TO *
150 ASSIGN# 3 TO *
160 DATA 6.912,6.805,6.663,6.534
    ,6.408,6.309,6.221,6.166,6.0
    83,5.916
170 REM .1356,.1386,.1437,.1537
    6,.1693,.1951,.1913,.1724,.1
    4412,.12466
180 FOR I=1 TO 10
190 READ C(I)
200 NEXT I
210 ON KEY# 1,"HI  F" GOSUB 280
220 ON KEY# 2,"MID F" GOSUB 370
230 ON KEY# 3,"LO F" GOSUB 460
240 ON KEY# 4,"Z" GOSUB 560
250 CLEAR @ KEY LABEL
260 DISP "SELECT OPTION"
270 GOTO 270
280 CLEAR
290 GOSUB 890
300 R=SQR(ABS(A0))
310 L=SQR(ABS(A1))
320 DISP "R IS ",R
330 DISP "L IS ";L
340 DISP "ENTER R,L"
350 INPUT R,L
360 RETURN
370 CLEAR @ GOSUB 890
380 R2=SQR(ABS(A0))-R
390 DISP "R2 IS ";R2
400 FOR I=S8 TO S9
410 C2=SQR(ABS(A1/((R^2-Z(I)^2)*
    R2^2)))
420 DISP "C2 IS ";C2
430 NEXT I
440 DISP "ENTER C2"
450 INPUT C2@ RETURN
460 CLEAR @ GOSUB 890
470 R1=SQR(ABS(A0))-(R+R2)
480 DISP "R1 IS ";R1
490 FOR I=S8 TO S9
500 C1=SQR(ABS(A1/(((R+R2)^2-Z(I
    )^2)*R1^2)))
510 DISP "C1 IS ";C1
520 NEXT I
```

```
530 DISP "ENTER C1"
540 INPUT C1
550 RETURN
560 CLEAR
570 DISP "FORMAT;C1,R1,R,L,C2,R2
    "
580 DISP C1,R1,R,L,C2,R2
590 DISP "ANY CHANGES Y/N"
600 INPUT A$
610 IF A$="N" THEN 640
620 DISP "INPUT C1,R1,R,L,C2,R2"
630 INPUT C1,R1,R,L,C2,R2
640 DISP "VAL TO CRT/PTR 1/2"
650 INPUT N
660 PRINTER IS N
670 PRINT L$
680 PRINT "FORMAT:C1,R1,R,L,C2,R
    2"
690 PRINT C1,R1,R,L,C2,R2
700 PRINT "FORMAT;REF Z,CALC Z"
710 FOR I=1 TO 10
720 W=2*PI*F(I)/1000000
730 C=C(I)*.000001
740 G1=1/R1 @ G2=1/R2
750 A1=G1^2+(W*C1)^2
760 A2=G2^2+(W*C2)^2
770 B=(R+G1/A1+G2/A2)^2
780 D=L-C1/A1-C2/A2
790 E1=(D/C)^2
800 E2=B/(W*C)^2
810 E3=W^2*(D-1/(W^2*C))^2
820 G=SQR(ABS((E1+E2)/(B+E3)))
830 PRINT Z(I);" ";G
840 NEXT I
850 DISP "ANOTHER RUN,Y/N"
860 INPUT O$
870 IF O$="Y" THEN 570
880 RETURN
890 REM WILL DO A SIMPLE LST SQR
    S FIT TO DATA
900 S1,S2,S3,S4=0
910 DISP "ENTER START PT,END PT
    FOR SUM"
920 INPUT S8,S9
930 S=S9-S8+1
940 FOR I=S8 TO S9
950 X=(2*PI*F(I)/1000000)^2
960 P=Z(I)^2
970 S1=S1+X
980 S2=S2+X^2
990 S3=S3+P
1000 S4=S4+P*X
1010 NEXT I
1020 Y1=S3/S1
1030 B1=S1*S1/(S2*S)
1040 Y2=S4/S2
1050 M1=S/S1
1060 A0=(Y1-Y2)/((1-B1)*M1)
1070 A1=Y1-A0*M1
1080 RETURN
```

81

APPENDIX E

SKIN EFFECT INDUCTANCE [Ref. 27]

To determine the inductance, the current distribution across the conductor must be determined.

Consider a cylindrical conductor of radius a, length ℓ, across sectional area A and conductivity Ko with current flowing along the long axis. The current is:

$$i(r) = I \frac{\text{Ber }(br) + j\text{Bei }(br)}{\text{Ber }(ba) + j\text{Bei }(ba)}$$

where $R = \ell/A\text{Ko}$, $b = (2\pi f\, uo\text{Ko})^{1/2} = \sqrt{\dfrac{f\text{Ko}}{355.9}}$

$$\text{Ber}(X) = 1 - \frac{(\tfrac{1}{4}X^2)^2}{(2!)^2} + \frac{(X^2)^4}{(4!)^2} - \ldots$$

$$\text{Bei}(X) = \frac{X^2}{4} - \frac{(\tfrac{1}{4}X^2)^3}{(3!)^2} + \frac{(\tfrac{1}{4}X^2)^5}{(5!)^2} - \ldots$$

1. Case I

For $r < a$, $a \cong .02$ or $.01m$, fmax = 10 Hz and Ko(max) = 10 s/m (characteristic of an electrolytic solution):

$$ba = 2.81 \times 10^{-5} \sqrt{\text{fmax Komax}}$$

$$= .281$$

which is less than 1, allowing all the higher order terms to be neglected. Thus we can say:

$$\text{Ber(ba)} \cong 1 \cong \text{Ber(br)}$$

and

$$\text{Bei(ba)} \cong \frac{(ba)^2}{4} \cong 0 \quad (.02 \text{ maximum})$$

Therefore the current is:

$$i(r) = \text{Io} \ \frac{1 + jo}{1 + jo} \cong \text{Io}$$

which imples the current is constant across the conductor cross-section.

2. Case II

For $r < u$, $u \cong .02$ or $.01$ m, fmax $= 10^7$ Hz, and Komax $= 10^7$ s/m, (characteristic of a metalic conductor):

$$ba = 2.81 \times 10^{-5} \ \sqrt{\text{fmax Komax}}$$

$$= 281$$

which is greater than 1, and emphasizes the higher order terms. Thus, the current will be contained almost entirely by the outer surface of the conductor.

The electrolytic solutions can be characterized by the development in Case I. The inductance (L) can be computed from:

$$\tfrac{1}{2}\text{L} \ i^2 = \int \frac{\mu}{2} \ H^2 \, dV$$

where u is the permeability and H is the magnetic field. For a cylindrical conductor of radius a, length h and uniform current distribution:

83

$$\tfrac{1}{2} L i^2 = h \int_0^a \frac{Uo}{2} \left(\frac{ir}{2\pi a^2}\right)^2 2\pi r dr = h\frac{\mu o i^2}{16\pi}$$

Thus, the inductance per unit length is:

$$\frac{L}{h} = \frac{Uo}{8\pi} = 5 \times 10^{-8} \ \frac{H}{m}$$

Therefore for an electrolytic solution in this configuration, with h = 10 m = .1m, the skin effect inductance is:

$$L = 5 \times 10^{-5} H = 5nH.$$

The zero offset adjustment (ZOA) is performed using mercury for the short circuit portion. Therefore, the skin effect inductance of mercury must be computed. Since the current in a mercury conductor is carried in the outer surface, as shown in Case II, it can be modeled as a plane conductor since the curvature is unimportant. The impedance of the strip of conductor of width d, and unit length is:

$$Z = \frac{E}{J} , \qquad E = \text{electric field}$$
$$J = \text{current per unit length}$$

$$= R + j\omega L$$

It can be shown that:

$$Z = \frac{(1 + j)}{Kodb}$$

Ko = conductivity, f = frequency

$$b = \frac{503.3}{\sqrt{fKo}}$$

84

Equating the imaginary parts of both expression:

$$j\omega L = j\frac{1}{Kobd} \qquad\qquad \omega = 2\pi f$$

the impedance becomes:

$$L = \frac{1}{\omega Kobd} = \frac{3.162 \times 10^{-4}}{d\sqrt{fKo}} \text{ H per unit length per unit width}$$

For $a \cong .01m$, $f = 10^4 - 10^7$ Hz, $Ko = 10^7$ and length $= .1m$,

$$L = \begin{cases} 1.6nH & f = 10^4 \text{ Hz} \\ .05nH & f = 10^7 \text{ Hz} \end{cases}$$

as the skin effect inductance for mercury.

LIST OF REFERENCES

1. Falkenhagen, H. and Debye, P., _Physik Z_, v. 29, p. 401, 1928.

2. Hamed, H. S. and Owen, B. B., _Physical Chemistry of Electrolytic Solutions_, Reinhold, 1963.

3. Condon, E. V. and Odishaw, H. (ed), _Handbook of Physics_, McGraw-Hill, 1963.

4. Smedley, S. T., _The Interpretation of Ionic Conductivity Liquids_, Plenum Press, 1980.

5. Fuoss, R. M. and Accoscina, F., _Electrolytic Conductance_, Interscience, 1959.

6. Falkenhagen, H., _Electrolyte_, S. Hirzel Verlag, Leipzig, 1953.

7. Sack, H., _Physiz, Z_, v. 29, p. 627, 1928.

8. Geest, Von H., _Physik, Z_, v. 34, p. 660, 1933.

9. Streetman, B. G., _Solid State Electronic Devices_, Prentice-Hall, 1972.

10. Jackson, J. D., _Classical Electrodynamics_, Wiley, 1962.

11. Becker, R., _Electromagnetic Fields and Interactions_, Blaisdell, 1964.

12. Kittel, C., _Introduction to Solid State Physics_, 3rd ed., Wiley, 1966.

13. Ibid, p. 392.

14. Hewlett-Packard letter HPON: 2700-34857 to Naval Postgraduate School, subject: _Certificate of Conformance_, 18 November 1982.

15. Hewlett-Packard Company, _Operating Manual Model 4275A Multifrequency LCR Meter_, 1982.

16. Harned, H. S. and Owen, B. B., _Physical Chemistry of Electrolytic Solutions_, Reinhold, 1963.

17. Hasted, J. B., Aqueous Dielectrics, Chapman-Hall, 1973.

18. Hewlett-Packard Company, HP-85 Owners Manual and Programming Guide, 1981.

19. Hornbeck, R. W., Numerical Methods, Quantum, 1975.

20. Smedley, SI, The Interpretation of Ionic Conductivity in Liquids, Plenum Press, 1980.

21. Falkenhagen, H., Electrolyte, S. Hirzel Vorkeg, 1953.

22. Walden, P., Z. Physik, Chem, v. 108, p. 341, 1924.

23. Hewlett-Packard Company, Operating Manual Model 4275A Multi-Frequency LCR Meter, 1982.

24. Hornbeck, R. W., Numerical Methods, Quantum, 1975.

25. Hewlett-Packard Company, HP-85 Owner's Manual and Programming Guide, 1981.

26. Harned, H. S. and Owen, B. B., Physical Chemistry of Electrolytic Solutions, Reinhold, 1963.

27. Ramo, S. and Whinnery, J. R., Fields and Waves in Modern Radio, Wiley, 1953.

INITIAL DISTRIBUTION LIST

No. Copies

1. Defense Technical Information Center   2
   Cameron Station
   Alexandria, Virginia 22314

2. Library, Code 0142   2
   Naval Postgraduate School
   Monterey, California 93940

3. Department Chairman, Code 61   1
   Department of Physics
   Naval Postgraduate School
   Monterey, California 93940

4. Professor J. R. Neighbours, Code 61Nb   1
   Department of Physics
   Naval Postgraduate School
   Monterey, California 93940

5. Dr. Michael E. Thomas   3
   The Johns Hopkins University
   Applied Physics Laboratory
   Johns Hopkins Road
   Laurel, MD 20707

6. John B. Kolbeck, LT, USN   2
   W186 N7125 Marcy Road
   Menomonee Falls, Wisconsin 53051